Petroleum Geology of the Sichuan basin, China--
Report on U.S. Geological Survey
and Chinese Ministry of Geology and Mineral Resources
field investigations and meetings, October 1991

Robert T. Ryder[1], Dudley D. Rice[2], Sun Zhaocai[3],
Zhang Yigang[3], Qiu Yunyu[3], and Guo Zhengwu[4]

Open-File Report 94-426

[1] U.S. Geological Survey, Reston, Virginia 22092
[2] U.S. Geological Survey, Denver, Colorado 80225
[3] Central Lab of Petroleum Geology, Ministry of Geology and
Mineral Resources, Wuxi, Jiangsu, China 214151
[4] Southwest Bureau of Petroleum Geology, Ministry of Geology and
Mineral Resources, Chengdu, Sichuan, China 610081

1994

CONTENTS

ILLUSTRATIONS

i

TABLES

APPENDICES

INTRODUCTION

Sichuan Province, particularly the Sichuan basin, is the most densely populated area in China and maybe the world (fig. 1). With the growing economy in China, they really have a need to expand their domestic energy sources. At present, China's economy is very dependent on coal which satisfies about 75% of its energy needs (Kruger, 1993). In contrast, natural gas, a good clean, efficient energy source, only represents less than 2% of China's energy use (Kruger, 1993). These averages are for all of China and the energy mix may be different for the Sichuan basin.

The Sichuan basin (fig. 1) is the leading gas producing basin in China (China Oil, 1987a; Oil and Gas Journal, 1992). The majority of the natural gas in the basin is nonassociated and is produced from carbonate reservoirs of Sinian, Paleozoic, and early Mesozoic age. Gas reservoirs commonly contain abundant tectonic fractures because of their association with highly compressed, thrust-faulted anticlines. Also, fractures produced by karst processes are common. Additional gas in the basin is produced from low-permeability Upper Triassic fluvial sandstone reservoirs and Permian and Triassic coal beds. Modest quantities of oil and associated gas are produced from lacustrine rocks of Jurassic age. Current exploration in the basin is limited to several wells a year that are drilled on the complexly folded and topographically rugged southeastern flank for deep (>3 km) nonassociated gas in fractured carbonate reservoirs.

In October 1991, geologists and geochemists from the U.S. Geological Survey (USGS) and the Chinese Ministry of Geology and Mineral Resources (CMGMR) met in Beijing, Chengdu, and Wuxi and at selected field localities to discuss the petroleum geology of the Sichuan basin. Through lectures and numerous field excursions, the Chinese hosts presented a wide array of current studies relevant to the Sichuan basin that included basin framework, source rock geochemistry, thermal maturation, and reservoir characterization. Ideas were freely exchanged on all topics but the Chinese seemed most interested in learning about the origin and habitat of coalbed gas and of natural gas in deep (>4.5 km) sedimentary basins. The USGS benefited greatly from this open dialogue and from the acquisition of maps, outcrop and subsurface samples of reservoir and source rock units, gas samples, and gas field production data. Most of this new information acquired by the USGS will augment existing literature compilations on the Sichuan basin by the World Energy Resource Program of the USGS (Lee and Masters, 1988; Ulmishek, 1993). Rice and Ryder found the Chinese geoscientists to be very adept at defining, investigating, and solving a wide range of petroleum exploration problems. They skillfully apply modern concepts and technology to petroleum exploration and where expertise is lacking in a particular discipline they seek competent consultants for data, advice, and training.

Figure 1. Map of the Sichuan Province, China showing the location of the Sichuan basin (Terrill, 1985).

2

This report is an overview of the petroleum geology of the Sichuan basin based largely on lectures, scientific dialogue and interpretations exchanged between USGS and CMGMR earth scientists. The report is organized by topics familiar to petroleum geologists with text and illustrations generally limited to current oil and gas developments in the basin and to published data, maps, and interpretations not readily available to foreigners.

Localities of natural gas, core, and outcrop samples, collected for geochemical analysis and study by USGS and CMGMR scientists, are listed in the report. The results of analyses of these samples are expected to be the subject of one or more scientific papers.

ACKNOWLEDGMENTS

GEOLOGIC FRAMEWORK

During the Paleozoic and early Mesozoic, the Sichuan basin occupied the western part of the Yangtze platform, a microcontinent whose constituent basement terranes had assembled between 850 and 700 Ma (Wang and others, 1989; Korsch and others, 1991). Shallow marine carbonate sedimentation began on the platform in Sinian time and lasted through Middle Triassic time. (See Table 1 for major geologic ages and orogenic events referred to in the text). Open ocean surrounded the Yangtze platform during most of the Paleozoic and early Mesozoic. The platform was affected by several epeirogenic events in the late Paleozoic that exposed large areas to subaerial conditions. Permian extension along the western margin of platform, possibly caused by back-arc spreading, produced a widespread outpouring of basaltic magma.

The Sichuan basin began to take shape during the early Mesozoic Indosinian orogeny (table 1) when the northwestern margin of the Yangtze platform collided with the Songpan-Ganzi block (Bally and others, 1986; Hsü and others, 1988). Subsequent Indosinian collisions of the Yangtze platform with the North China-Korean block on the north and with Tibet on the west, firmly amalgamated the Yangtze microcontinent to the Eurasian plate. Compressional tectonism during the late Mesozoic Yanshanian orogeny and the

Geological Chronology			Age Ma.	Tectonic stages
CENOZOIC	Quaternary	Q4		L. Himalayan
		Q3		
		Q2		
		Q1	2.0	
	Tertiary	N2	24.6	M. Himalayan
		N1		
		E3		E. Himalayan
		E2		
		E1	65	
MESOZOIC	Cretaceous	K3		L. Yanshanian
		K2	104	M. Yanshanian
		K1		
	Jurassic	J3		E. Yanshanian
		J2		
		J1		
	Triassic	T3	213	Indo-Sinian
		T2		
		T1		
PALAEOZOIC	Permian	P2	248	Variscan
		P1	286	
	Carboniferous	C3		
		C2		Tienshanian
		C1	360	
	Devonian	D3		
		D1 – 2	408	Caledonian
	Silurian	S2 – 3		
		S1	438	
	Ordovician	O3		Taconian
		O1 – 2	505	
	Cambrian	$\mathcal{E}$2 – 3		Hsingkaiian
		$\mathcal{E}$1	590	
PROTEROZOIC	Sinian	$Pt_3 \frac{Z2}{Z1}$	700	Yangtzeian
			850	
	Chingpaikou		1000	
	Chihsien	Pt_2	1400	
	Changcheng			
	Hufo	Pt_1	1700	Chungtiaoian
Arch-aean	Watai		2000	Wutaian
	Fuping	Ar	2500	Fupingian

Table 1. Geologic time scale, stratigraphic intervals, and tectonic events in China (Cheng and others, 1986).

Tertiary Himalayan orogeny (table 1) completed the conversion of the stable marine carbonate platform to a continental basin.

Topographically, the Sichuan basin is a conspicuous depression, ranging in elevation from 1,000 to 2,000 m, surrounded by rugged mountainous terrain. The southeastward flowing Min, Tuo, Fu and Jialing Rivers, from which the Province and basin derive their name (four rivers), originate in the high mountains of northern Sichuan Province, cross the fertile alluvial plain of the basin, and join the northeastward-flowing Chang Jiang (Yangtze River) along the southeastern flank of the basin (fig. 1). In ancient times the basin was accessible only from the north along the Jialing Jiang (River) and from the east along the Chang Jiang (River).

In outcrop, the Sichuan basin is a northeasterly trending, trapezoid-shaped, structural depression--600 km long by 380 km wide-- filled with gently dipping to tightly folded, nonmarine strata of Mesozoic age (fig. 2). The basin is flanked by orogenic belts containing plutonic and metamorphic rocks of Proterozoic and early Paleozoic age and marine strata of latest Proterozoic (Sinian), Paleozoic, and early Mesozoic age (fig. 2). Three major structural provinces are recognized in the basin: 1) a northeast-trending central uplift, 2) a foredeep (northwestern depression) on the northwest side and 3) a fold belt (southeastern fold belt) on the southeast side (fig. 3).

The foredeep is characterized by an eastward-thinning, 12-km-thick sedimentary wedge that consists of about 4 km of shelf and continental margin carbonates of Sinian through Middle Triassic age and about 8 km of fluvial and lacustrine rocks of Late Triassic through Cretaceous age. A generalized stratigraphic column for the Sichuan basin is illustrated in figure 4. In the vicinity of Chengdu (figs. 2,3), the Cretaceous strata of the foredeep are overlain by a 500-m-thick deposit of Pliocene-Quaternary sand and gravel. The Longmenshan fold and thrust belt, containing thick thrust slices of Proterozoic granitic basement and Paleozoic sedimentary rocks, adjoin and override the foredeep on the northwest (fig. 5). The major level of detachment in the frontal zone of the Longmenshan fold and thrust belt occurs in Sinian and(or) Cambrian strata. Basinward, these bedding plane thrusts cut upsection, across several ramps, to successively younger strata in the foredeep. Imbricate thrusts, ramp anticlines, blind thrusts, and triangle zones are typical structures observed in this belt of decollement tectonics in the northwestern margin of the Sichuan basin (fig. 5).

The first major orogenic phase (Indosinian orogeny; table 1) of the Longmenshan fold and thrust belt occurred when the northwest margin of the Yangtze platform collided with the Songpan-Ganzi block (Bally and others, 1986; Hsü and others, 1988). Between 3,000 and 4,000 m of Late Triassic fluvial sandstone and shale, derived from a northwestern source area, were deposited in the adjoining

5

Figure 2. Geologic map of Sichuan Province, China and adjoining provinces showing the Sichuan basin and its folded and thrust-faulted margins (Huang, J.Q. and others, 1976). The explanation is on the following page.

EXPLANATION (for figure 2)

Geologic Period | **Sedimentary rocks** | **Igneous rocks** | **Other**

Geologic Period	Sedimentary rocks
Quaternary	Q
Neogene and Paleogene	N - E
Cretaceous	K
Mesozoic — Jurassic	J_3
	J_2
	$T_3 - J_1$
Triassic	T_3
	T_2
	T_{1+2}
	T_1
	P + T
Paleozoic — Permian	P / P_2 / P_1
	P + C
Carboniferous	C
	D + C
Devonian	D
	S + D
Silurian	S
	O + S
Ordovician	O
	ε + O
Cambrian	ε
Proterozoic — Sinian	Z / Z_{Z2} / Z_{Z1} / Z_Z
	P_{t2}
Pre-Sinian	Zci
	P_{t1}

P_{Z2} P_{Z1}

Igneous rocks

γ_5 Granite ε_5 Syenite

σ_5 Pyroxenite

$\ulcorner P \urcorner$ Basalt

ζ_3 Alkaline porphyry

V_4 Gabbro

γ_3 Granite φ_3 Diabase

γ_2 Granite δ_2 Diorite β_2 Diabase V_2 Gabbro

Other

River

Fault

Strike-slip Fault

Line of Section

● Nuji Nuji well

▲ Outcrop Section

C. Chongqing area
Gx. Guanxian area
E. Emeishan area
G. Guangyuan area

Major strike-slip Fault systems

AF. Anninghe fault
XF. Xianshuihe fault
ZF. Zumuhe fault

⊙ City

B. Bazhou
C. Chengdu
Cq. Chongqing
Gy. Guangyuan
H. Hangzhong
K. Kangding
L. Leshan
Lu. Luzhou
M. Mianyang
N. Neijiang
Na. Nanchong
W. Wanxian
X. Xichang
Y. Ya'an
Yi. Yibin
Yic. Yichang
Z. Zigong

Figure 3. Map of the Sichuan basin showing oil and gas fields and major structural provinces.

8

Era	System	Series	Formation	Age Symbol	Age (Ma)	Lithology	Thickness (m)	Lithologic Description	Reservoir	Source Rock	Seal
Cenozoic	Quat.			Q	3		0-380	Gravel, sand, clay			
Cenozoic	Neogene			N	25		0-300	Conglomerate, sandstone			
Cenozoic	Paleog.			E	80		0-800	Brownish-red mudstone, siltstone, sandstone			
Mesozoic	Cret.			K	140		0-2000	Brownish-red mudstone, sandstone, sandy conglomerate, marlstone			
Mesozoic	Jurassic	Upper	Penglaizhen Fm.	J3p			650-1400	Gray sandstone, red mudstone, conglomeratic sandstone			S
Mesozoic	Jurassic	Upper	Suining Fm.	J3sn			340-500	Red mudstone, siltstone			
Mesozoic	Jurassic	Middle	Shaximiao and Qianfoya Fms.	J2s J2q			600-2800	Red and green mudstone, sandstone, dark gray shale, and mudstone		□	S
Mesozoic	Jurassic	Lower	Ziliujing Fm.	J1z	195		200-900	Gray shale, marlstone, shelly limestone	O O	□	
Mesozoic	Triassic	Upper	Xujiahe Fm.	T3x	205		250-3000	Dark-gray shale, sandstone, coal	☼ts ☼cb	▷	
Mesozoic	Triassic	Middle	Leikoupo Fm.	T2l				Limestone, dolomite, anhydite	☼		S
Mesozoic	Triassic	Lower	Jialingjiang Fm.	T1j			900-1700	Limestone, dolomite, anhydrite	☼		S
Mesozoic	Triassic	Lower	Feixianguan Fm.	T1f	230			Red shale, red mudstone, micritic limestone	☼		S
Paleozoic	Permian	Upper	Talung & Wujiaping Fms.	P1			200-500	Limestone, shale, coal	☼ ☼cb	□ ▷	
Paleozoic	Permian	Lower	Maokou and Qixia Fms.	P2	270		200-500	Limestone, black shale	☼		
Paleozoic	Carbonif.			C	320		0-500	Dolomite, limestone	☼		
Paleozoic	Silurian	Middle		S2			50	Green shale, calcareous sandy siltstone			S
Paleozoic	Silurian	Lower		S1			400-900	Black shale, silty sandstone		□	S
Paleozoic	Ordov.			O			252-615	Limestone, shale, sandstone			
Paleozoic	Cambrian			E2-3			220-420	Limestone, shale			S
Paleozoic	Cambrian			E1	570		225-900	Black shale, siltstone, sandy mudstone		□	
Proterozoic	Sinian	Upper		Z2			200-1100	Dolomite with stromatolites, shale	☼		
Proterozoic	Sinian	Lower		Z1	850		0-400	Sandy conglomerate, shale, andesite, rhyolite, tuff			
Proterozoic	pre-Sinian			AnZ				Slate, marble, phyllite, granite			

Legend:

Oil Reservoir — O
Gas Reservoir — ☼
Tight-sandstone gas reservoir — ☼ts
Coalbed gas reservoir — ☼cb
Source Rock, oil prone — □
Source Rock, gas prone — ▷
Seal — S

Figure 4. Generalized stratigraphic column for the Sichuan basin showing major oil and gas reservoirs, source rocks, and seals.
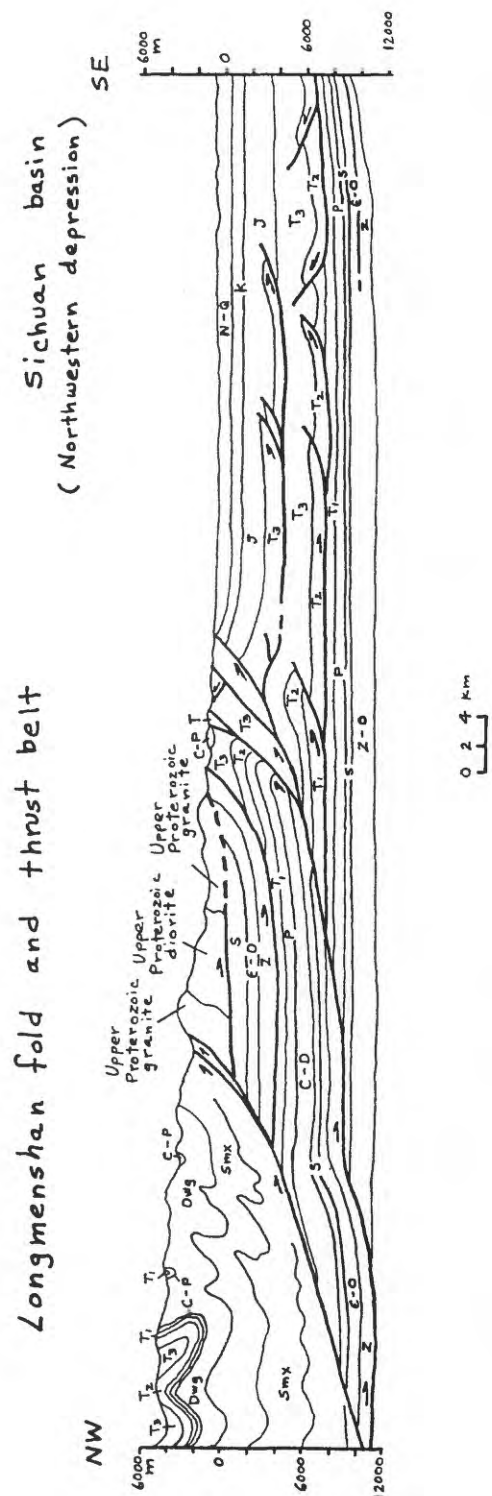
Figure 5. Geologic cross section through the Longmenshan fold and thrust belt and the northwestern Sichuan basin (Song Wenhai, 1989). The line of section is located in figure 2.

Sichuan basin foredeep (Bao and others, 1985; Guo, 1991a). Decollement tectonics that involve the lower Paleozoic strata in the frontal zone of the Longmenshan fold and thrust belt and Mesozoic strata in the Sichuan basin foredeep primarily resulted from the Himalayan orogeny of Tertiary age (table 1).

The central uplift is marked in outcrop by Jurassic rocks that dip gently northwestward into the foredeep from the adjoining frontal anticlines of the southeastern fold belt (fig. 2). Cretaceous strata undoubtedly were deposited across part or all of the central platform but have been removed by post-orogenic uplift and erosion. Jurassic strata and underlying Upper Triassic strata on the central platform are nonmarine in origin and have a combined thickness of about 2.5 km. This Upper Triassic and Jurassic sequence is underlain by about 3.5 km of Sinian to Middle Triassic platform carbonates. Many of the Lower and Middle Triassic carbonates are interbedded with evaporites. Widespread pre-Permian uplift and erosion have removed most of the Silurian, Devonian, and Carboniferous sequences from the central uplift (Bao and others, 1985; Guo, 1991a). Broad, basement-involved anticlines with locally faulted flanks, such as the Weiyuan anticline northwest of Zigong (figs. 2,3), characterize the dominant structural style of the central uplift. Anticlinal structures at the southern end of the central uplift may be detached along bedding plane thrusts in Cambrian strata.

The southeastern fold belt consists of long, tightly compressed anticlines typical of decollement-style tectonics. In outcrop, the anticlines are marked by conspicuous linear ridges of Triassic and Jurassic fluvial sandstone and the intervening synclines are marked by Jurassic lacustrine and fluvial shale (fig. 2). Detachment has occurred along a basal sole thrust in Cambrian shale and, to a lesser degree, along bedding plane thrusts in Triassic evaporites (fig. 6). Commonly, anticlinal cores have been disrupted by thrust faults. The thickness of strata in the southeastern fold belt is about 7.5 km. The sedimentary sequence in this structural province is about 1.5 km greater than the sequence in the central uplift largely because of the increased thickness of Cambrian and Silurian rocks and the addition of Carboniferous and Devonian rocks.

The southeastern fold belt of the Sichuan basin is the frontal zone of a large fold and thrust belt that extends into adjoining Guizhou and Hunan Provinces. This orogenic belt has been assigned a variety of names: 1) Qiyaoshan fold belt (Sun and others, 1991), 2) Guizhou folded belt (Hsü and others, 1988), and 3) Hubei-Guizhou platformal fold belt (Bao and others, 1985). Geologic cross sections through the Qiyaoshan fold belt (name preferred here) and the adjoining southeastern fold belt show increasingly complex structural patterns from northwest to southeast (figs. 6,7). Northwest verging, imbricate thrust sheets and anticlines, involving Cambrian through Permian strata, are exposed throughout the Qiyaoshan fold belt whereas thick thrust slices containing Proterozoic metasedimentary
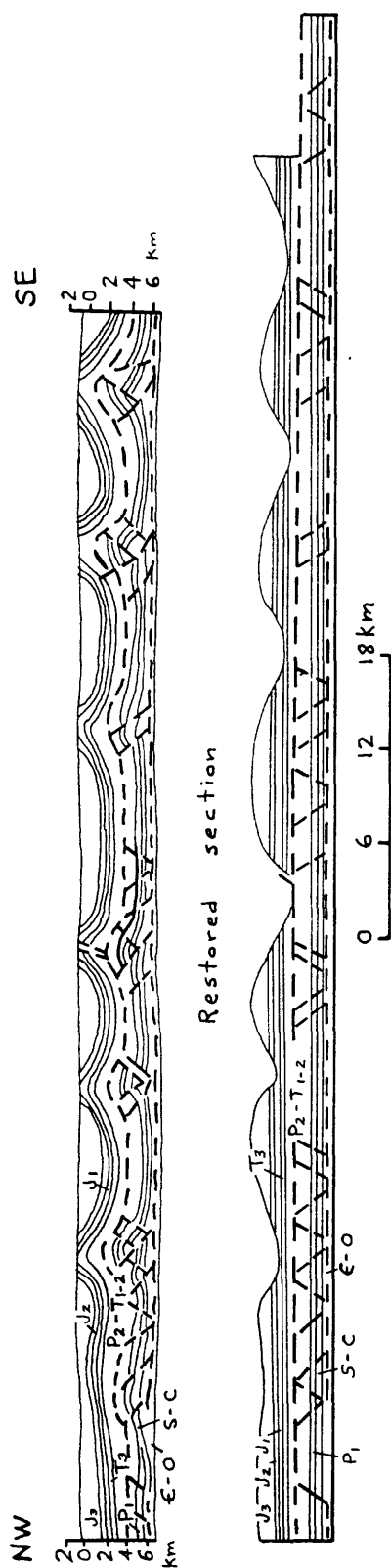
Figure 6. Geologic cross section through the southeastern fold belt of the Sichuan basin (Liu Hefu, 1989). The line of section is located in figure 2.

NW

SE

Sichuan basin

Central platform

Southeastern fold belt

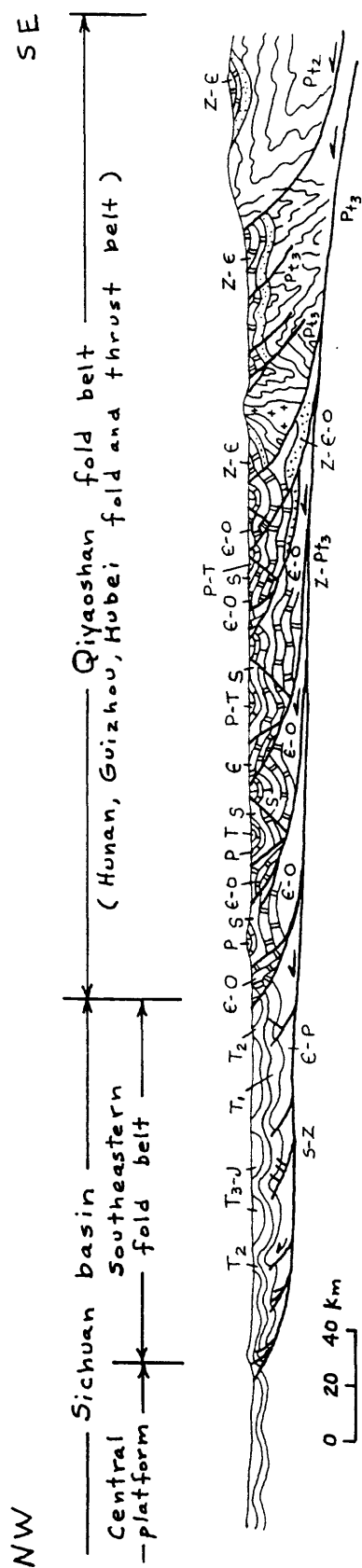Qiyaoshan fold belt

(Hunan, Guizhou, Hubei fold and thrust belt)

Figure 7. Geologic cross section through the southeastern part of the Sichuan basin and the adjoining Qiyaoshan fold belt (Sun and others, 1991). The line of section is located in figure 2.

13

rocks, local intrusive rocks, and Sinian and Cambrian sedimentary
rocks are confined to the rear of the thrust belt (fig. 7).

The Micangshan and Dabashan fold and thrust belts border the
northeast flank of the Sichuan basin (figs. 2,3). They are similar
to the Longmenshan orogenic belt in that thick thrust slices of
Proterozoic plutonic and metamorphic basement rocks, with a cover of
Sinian and lower Paleozoic sedimentary rocks, have been juxtaposed
against a foredeep containing Jurassic and Cretaceous continental
strata. Anticlines in the adjoining Jurassic foredeep and underlying
platform carbonates are underlain by imbricate thrusts that have
propagated southward and upsection from a zone of basal detachment in
Cambrian shale (Sun and others, 1991). The northwesterly to westerly
trending structures of the Micangshan and Dabashan fold and thrust
belts and the similar trending frontal folds and imbricate thrusts in
the Sichuan basin are strongly divergent from the dominant northeast
structural grain of most of the basin.

The southwestern margin of the Sichuan basin is bordered by the
north-trending Xichang-Yunnan fold and thrust belt (figs. 2,3; Bao
and others, 1985) which has had a complex history of extensional,
compressional, and strike-slip tectonics. The west side of the
tectonic belt is constrained by the active Xianshuihe and Anninghe
fault zones--Kangdian suture of Hsü and others, (1988)--which
constitute part of a 1,400 km-long left-lateral fault system that
extends from southern Qinghai Province to southern Yunnan Province
(fig. 2; Allen and others, 1991). Broad north-trending anticlines,
basement involved east-verging thrust faults, and normal faults later
converted to strike-slip faults characterize the complex array of
structures in the Xichang-Yunnan fold and thrust belt (Chen and Chen,
1987; Chou and Liu, 1988; Liu, 1988). The sedimentary record in the
Xichang-Yunnan fold and thrust belt consists of 1) Sinian and lower
Paleozoic carbonate and terrigenous clastic rocks of marine origin
deposited in an intraplatformal depression, 2) Permian basalt and
overlying platform carbonates, 3) Lower and Middle Triassic marine
carbonates and nonmarine terrigenous clastic rocks, and 4) 4- to 5-
km-thick Upper Triassic through Cretaceous nonmarine sandstone and
shale deposited in a foredeep contiguous with the Longmenshan
foredeep (northwestern depression).

Hsü (1989) speculates that widespread Permian rifting and
associated basaltic flows may reflect back-arc spreading between the
western Yangtze platform and an island arc located west of the
platform. Foreland basin sedimentation and compressional tectonics,
caused by the collision of the Yangtze platform with eastern Tibet,
dominated the Xichang-Yunnan fold and thrust belt from Late Triassic
through the Cretaceous and created the north-trending structural
grain. Left-lateral strike slip along the Xianshuhe fault zone and
reactivated faults in the Xichang-Yunnan fold and thrust belt was
introduced during the Himalayan orogeny.

14

Thick Pliocene-Quaternary deposits of the Chengdu plain indicate that the foredeep part of the basin is still subsiding. However, most of the Sichuan basin has experienced between 2 and 5 km of post-orogenic uplift and erosion in the past 10 million years.

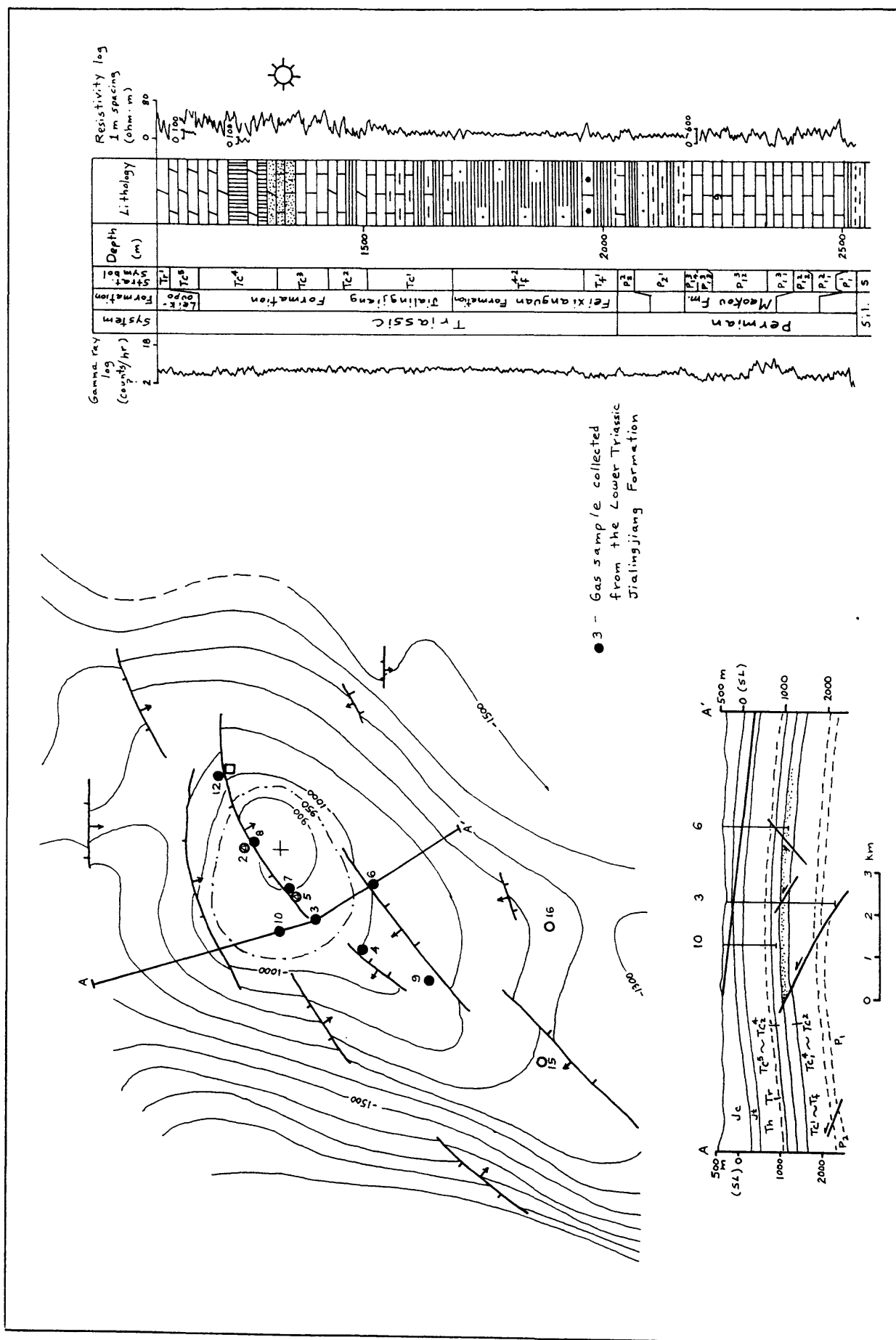## DISTRIBUTION OF OIL AND GAS FIELDS

The majority of the nonassociated natural gas produced to date in the Sichuan basin is trapped in tightly compressed, faulted anticlines in the southeastern fold belt and the southwestern part of the central uplift (fig. 3). Reservoirs in these fields consist of shallow marine limestone and dolomite of Carboniferous, Permian, and Lower and Middle Triassic age with fracture, vuggy, intergranular, and intercrystalline porosity. Lower and Middle Triassic evaporites are important seals. Drilling depth to most fields average 3,500 m and as of 1988 the deepest well was 7,175 m (Ma and Wu, 1988). Several of these fields are shown in figures 8, 9, and 10. Details of the decollement-style tectonics recognized in gas fields of the southeastern fold belt are described by Bao and others (1985), Xu (1988), and Lu and others (1989).

Nonassociated natural gas also is trapped in faulted anticlines in the northwestern depression (fig. 3). The Hewangchang gas field produces from Lower and Upper Permian limestone whereas the Zhongba gas field produces from Middle Triassic dolomite and Upper Triassic sandstone (figs. 11,12). Structural details of the Zhongba gas field are discussed by Chen and others (1992).

The giant Weiyuan gas field is located at the southwest end of the central uplift (fig. 3). This field differs from the previously mentioned fields because of its broad, open, anticlinal geometry and the structural involvement of pre-Sinian basement rocks (fig. 13). Fractured, shallow marine carbonates of Late Sinian age constitute the reservoir and Cambrian mudstone provides the seal (Korsch and others, 1991).

Most of the oil discovered to date in the Sichuan basin is located on the central uplift in broad open anticlines and stratigraphic traps (fig. 3). The reservoirs consist of lacustrine limestone and fluvial sandstone of Early and Middle Jurassic age (Yin, 1985; Zhai and others, 1987). Figure 14 shows the Nanchong oil field where the oil is trapped in a northwest-trending anticline. The Guehua oil field is primarily a stratigraphic-trap accumulation perched on a structural terrace (fig. 15).

In the late 1980's, deep drilling in the northwestern depression near Deyang discovered gas in fractured Upper Triassic sandstone at a depth of about 4.7 km. The gas, which initially tested at 1 million m^3/day, is trapped in an east-verging, highly faulted anticline with detachment in the Middle Triassic sequence. Guo (1991b) interprets the low permeability and abnormally high pressure of the producing

15

Figure 8. Structure contour map and cross section of the Xinglongchang gas field. The field is located on figure 3.

Figure 9. Structure contour map and cross section of the Ziliujing gas field. The field is located on figure 3.
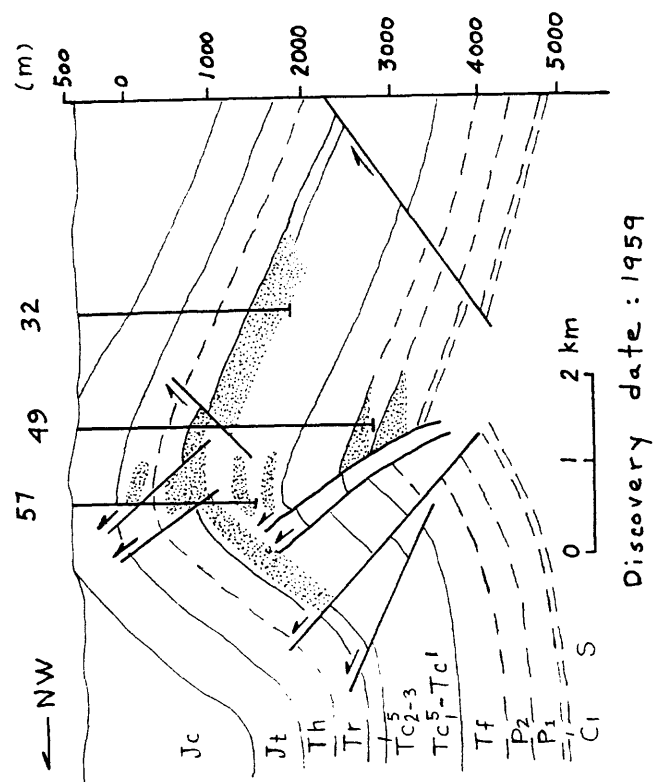
Figure 10. Cross section through the Wolonghe gas field (Gas fields of China, 1987). The field is located on figure 3.

Figure 11. Structure contour map and cross section of the Hewangchang gas field. The field is located on figure 3.

19

Figure 12. Structure contour map and cross section of the Zhongba gas field. The field is located on figure 3.

Figure 13. Structure contour map and cross section of the Weiyuan gas field. The field is located on figure 3.
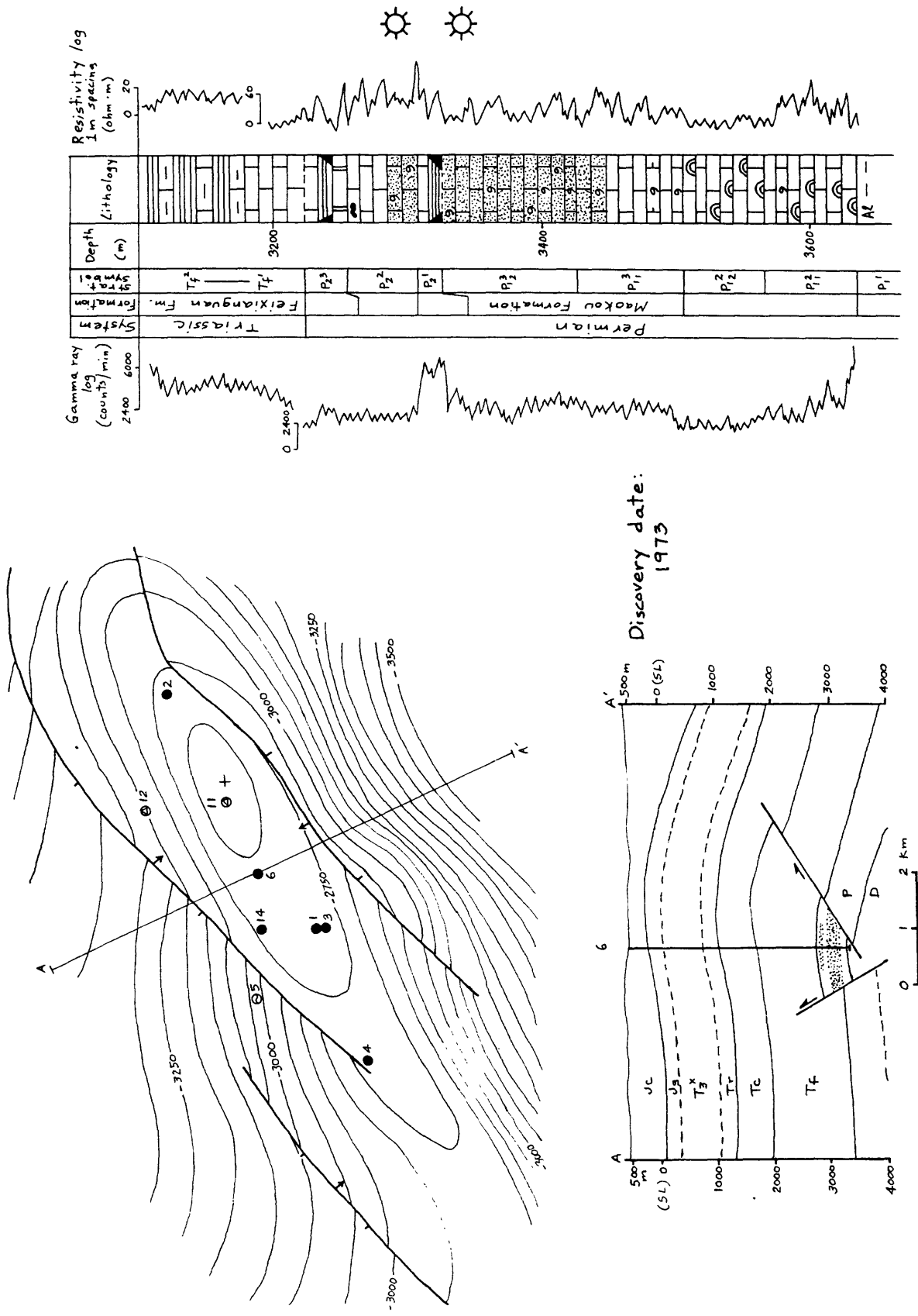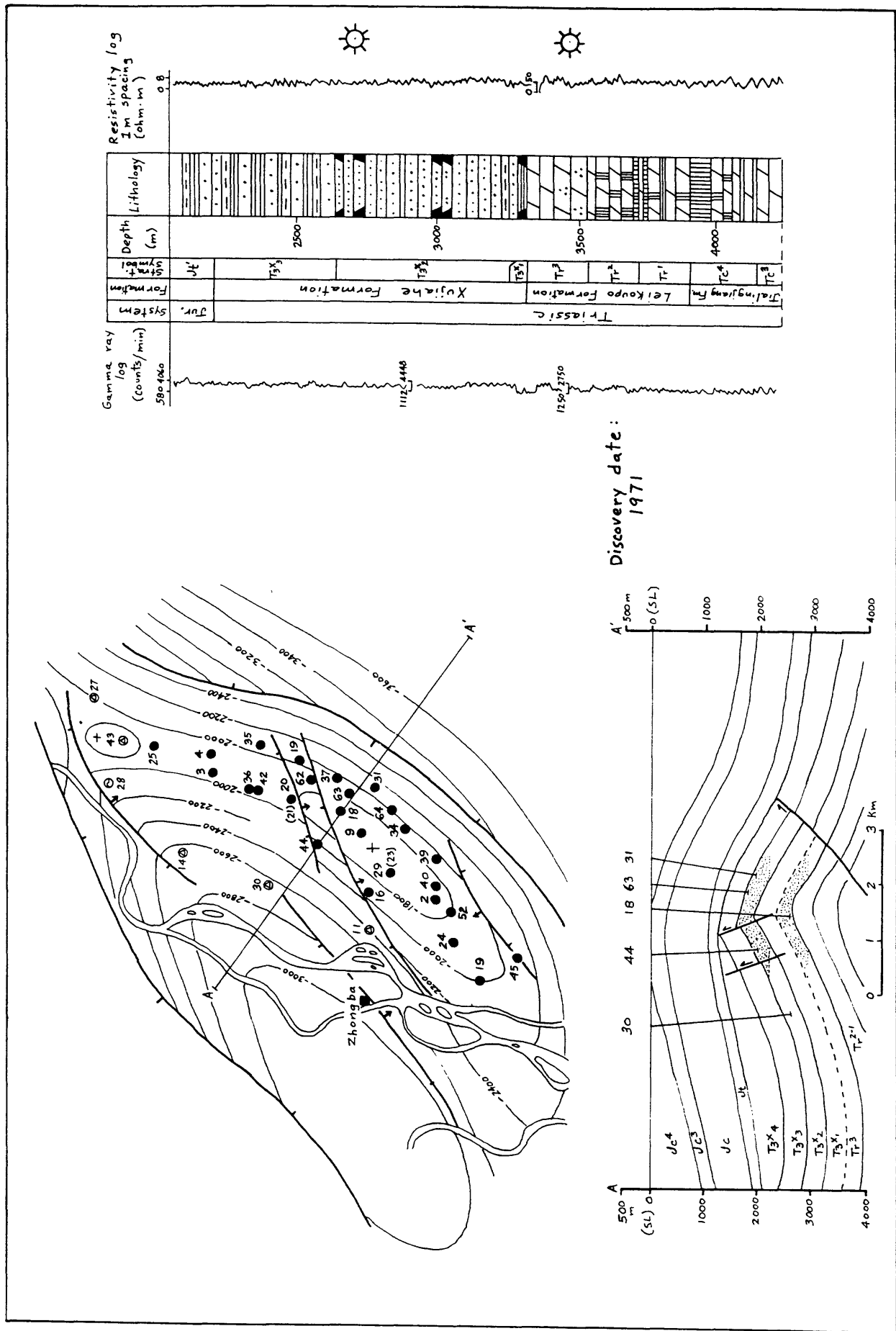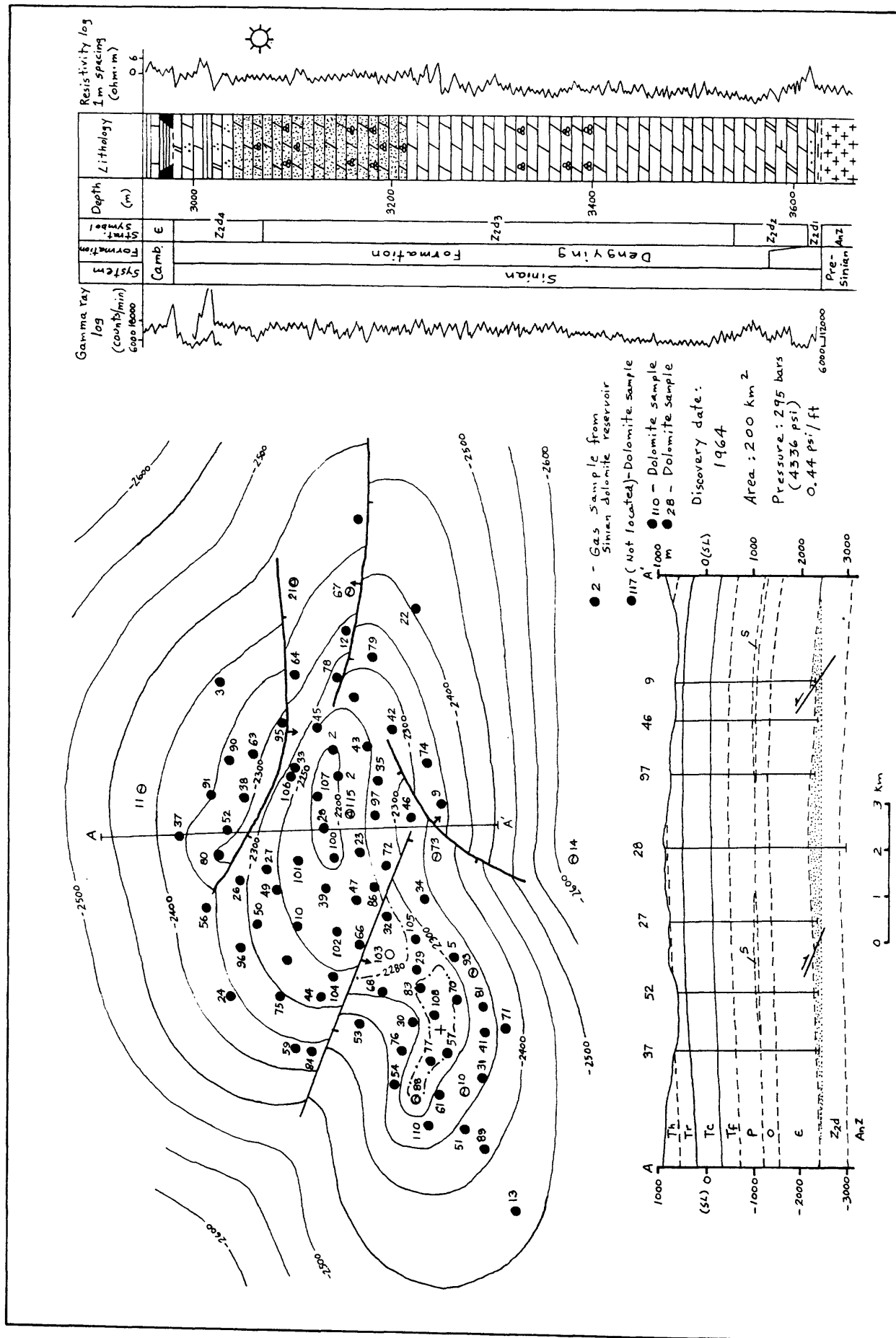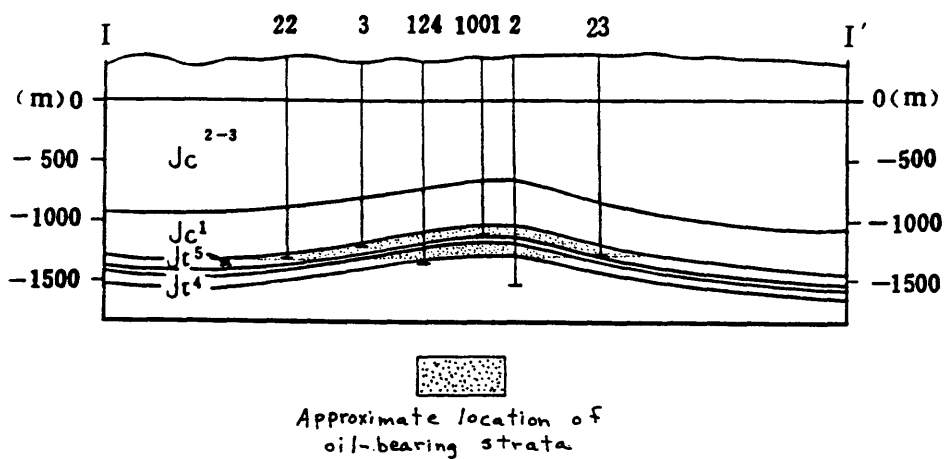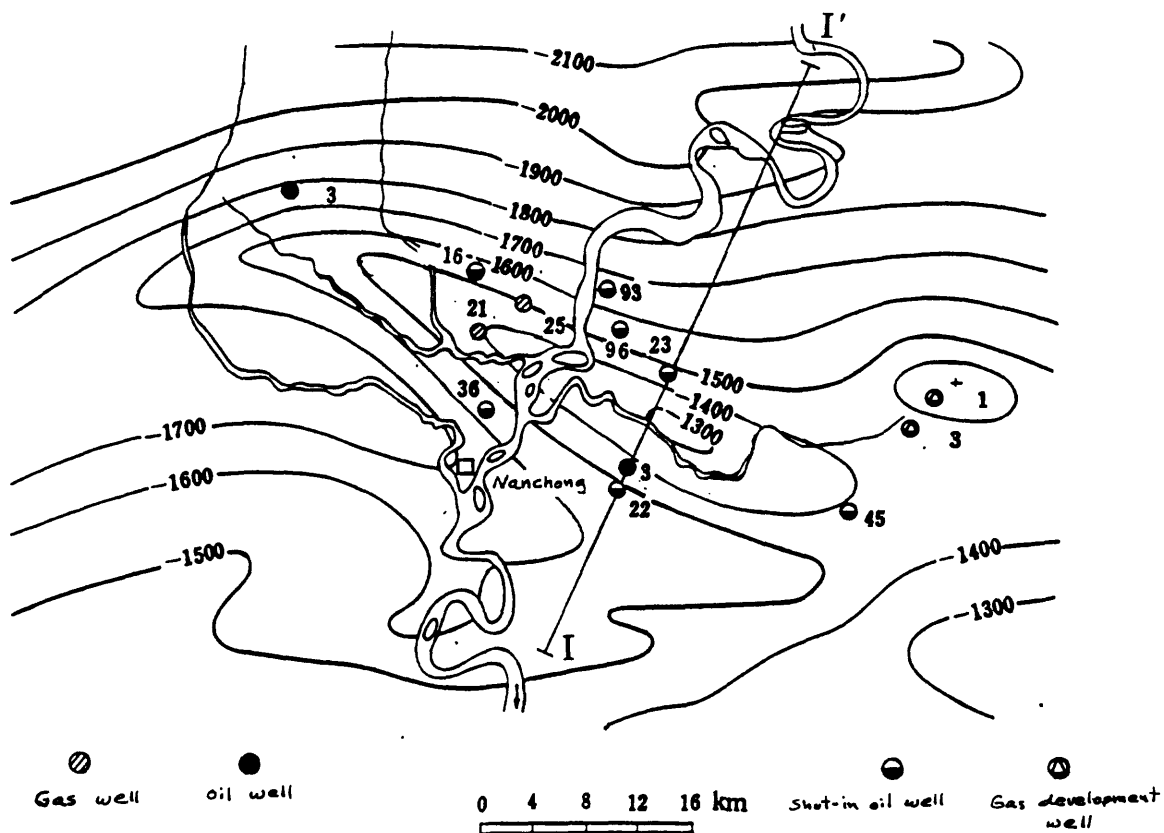
21

Figure 14. Structure contour map and cross section of the Nanchong oil field (Zhai and others, 1987). The field is located on figure 3.
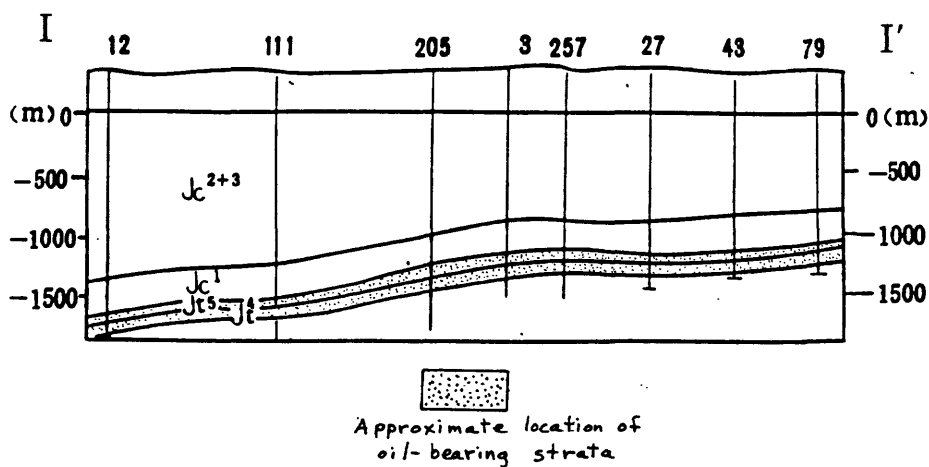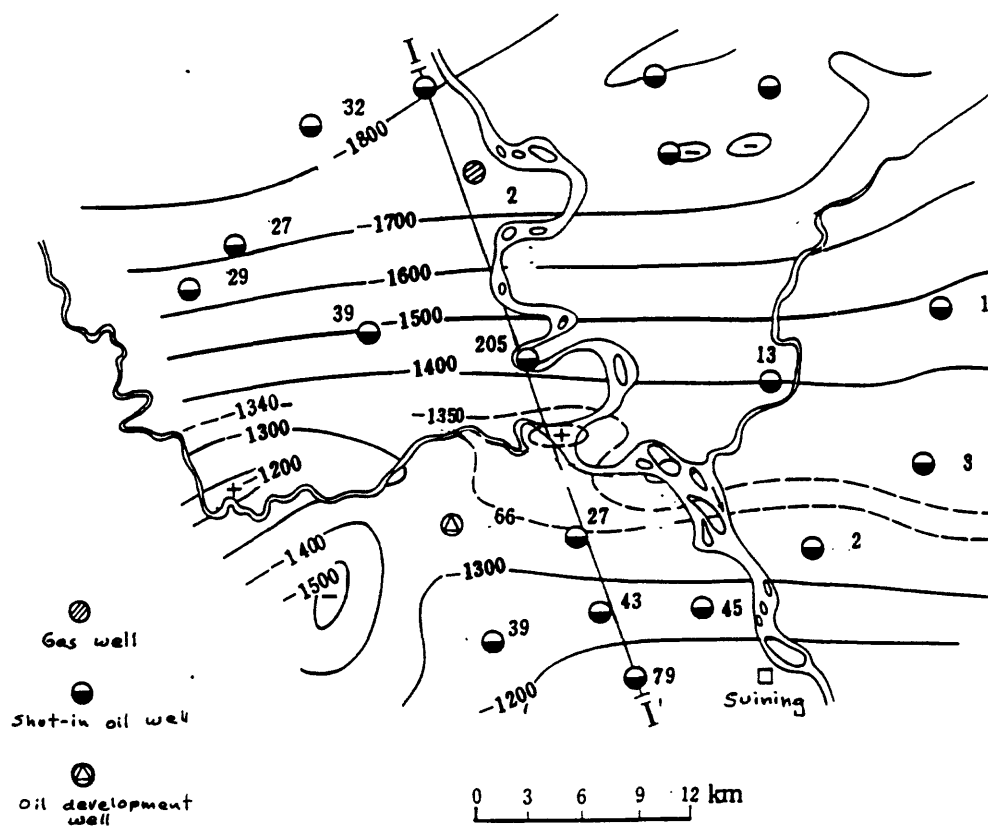
Figure 15. Structure contour map and cross section of the Guehua oil field (Zhai and others, 1987). The field is located on figure 3.

sandstones to be indicative of a tight sandstone reservoir. Although
not fully evaluated, these tight sandstone reservoirs could represent
a basin-center gas accumulation with substantial reserves.

Small amounts of coalbed gas are produced in the Sichuan basin
(China Oil, 1986). Most of the produced coalbed gas comes from a
fig. 13150-m-thick, coal-bearing interval at the base of the Upper
Permian in the southeastern fold belt. Individual coal beds are 1 to
2 m thick. Nantong, Tianfu, Zhongliangshan, and Songzao are some of
the gassy mining areas (administrations) which are located in the
southeastern fold belt near Chongqing. Widespread Upper Triassic
coalbeds are a source of local coalbed gas in the northwestern
depression (Dai, 1980).

China is the world's largest producer of coal (>1 billion
tons/year) and is also the largest emitter of coalbed methane because
most of their coal is mined underground. In addition, the methane
causes serious hazards (outbursts and explosions) which endanger the
miners' lives. So by recovering more of the coalbed gas, they would
add reserves of a clean energy source, cut down on greenhouse gas
emissions, and reduce mining hazards. In 1990, China recovered about
15 billion cubic feet of coalbed gas by mine degasification systems
(Kruger, 1993). About 65% of this recovered gas was used, mostly by
residences in the vicinity of the mines (Kruger, 1993). In the
future, coalbed gas reserves could be increased by improving recovery
and utilization in the mining areas and by exploration in the deeper
parts of the basin away from the mining areas. The recoverability of
the gas from the coal may be adversely affected by the multiple
stages of tectonic activity which have resulted in reduced
permeability. In addition, the general high rank of the coal is not
favorable for the preservation of permeability. Therefore, the best
prospects for coalbed gas will probably be in the mining areas where
the gas has to be removed to make for safer mining conditions and to
cut down on pollution.

RESERVOIR CHARACTER, PRESSURE, AND TEMPERATURE

Reservoir character is based on observations made at four
outcrop sections: 1) Guangyuan area along the Jialing Jiang about 5
km north of Guangyuan and the Shangxi about 15 km southwest of
Guangyuan (fig. 16), 2) Guanxian area along the Min Jiang (fig. 17),
3) Emeishan area (fig. 18) and 4) Chongqing area (fig. 19) along the
Jialing Jiang. These four outcrop localities are identified in
figures 2 and 3. Although these outcrop sections are tens of
kilometers from the oil and gas fields, they provide pertinent
reservoir data such as lithology, depositional history, bedding
structure and geometry, porosity types, and mineral composition of
grains and cement. Most outcrops are well exposed except for those
in the Dujiangyan area where dense forests and vegetation obscure
detailed observations. Moreover, evaporite-bearing zones in outcrop
sections in the Guangyuan, Emeishan, and Chongqing areas have been

Figure 16. Generalized stratigraphic section of parts of the Carboniferous, Permian, Triassic, and Jurassic sequence, Guangyuan area, Sichuan. The Triassic and Jurassic parts of the section are located along the Jialing Jiang north of Guangyuan, whereas the Carboniferous and Permian parts of the section are located in the Shangxi area southwest of Guangyuan. Described October 10-12, 1991. See Appendix C for explanation.

25

The figure shows a generalized stratigraphic section. Labels within the column (left to right columns):

Triassic / Upper (T₃) / Xujiahe Formation (T₃x) / Member

Approximate thickness (m) — 0

Member 4

sample Gx-6

1000

very immature, dk. colored lithic arenite, v. argillaceous, low porosity, m.- crs. grained with carbonaceous fragments. Coal beds (as many as 8 coal beds mined here but due to thrusting there may be repetition)

type 3 kerogen sample Gx-7

Sample -5

Member 3

2000

Sample Gx-3

Member 2

main reservoir interval; covered in this section; reported to be cleaner with fewer lithic fragments than member 3; secondary intergranular porosity in subsurface

3000

sample Gx-4

Member 1

Lower Permian rocks exposed in Klippe infolded with Upper Triassic rocks

Permian / Lower (P₁) / Qixia Formation

Approximate thickness (m) — 0

sample Gx-1

100

sample Gx-2

Triassic / Upper (T₃) / Xujiahe Formation / mbr. 3

Figure 17. Generalized stratigraphic section of parts of the Permian and Triassic sequence, Guanxian area, Sichuan. Described October 14, 1991. The stratigraphy of the Upper Triassic sequence is not fully resolved because of complex structure and poor exposures. See Appendix C for explanation.

26
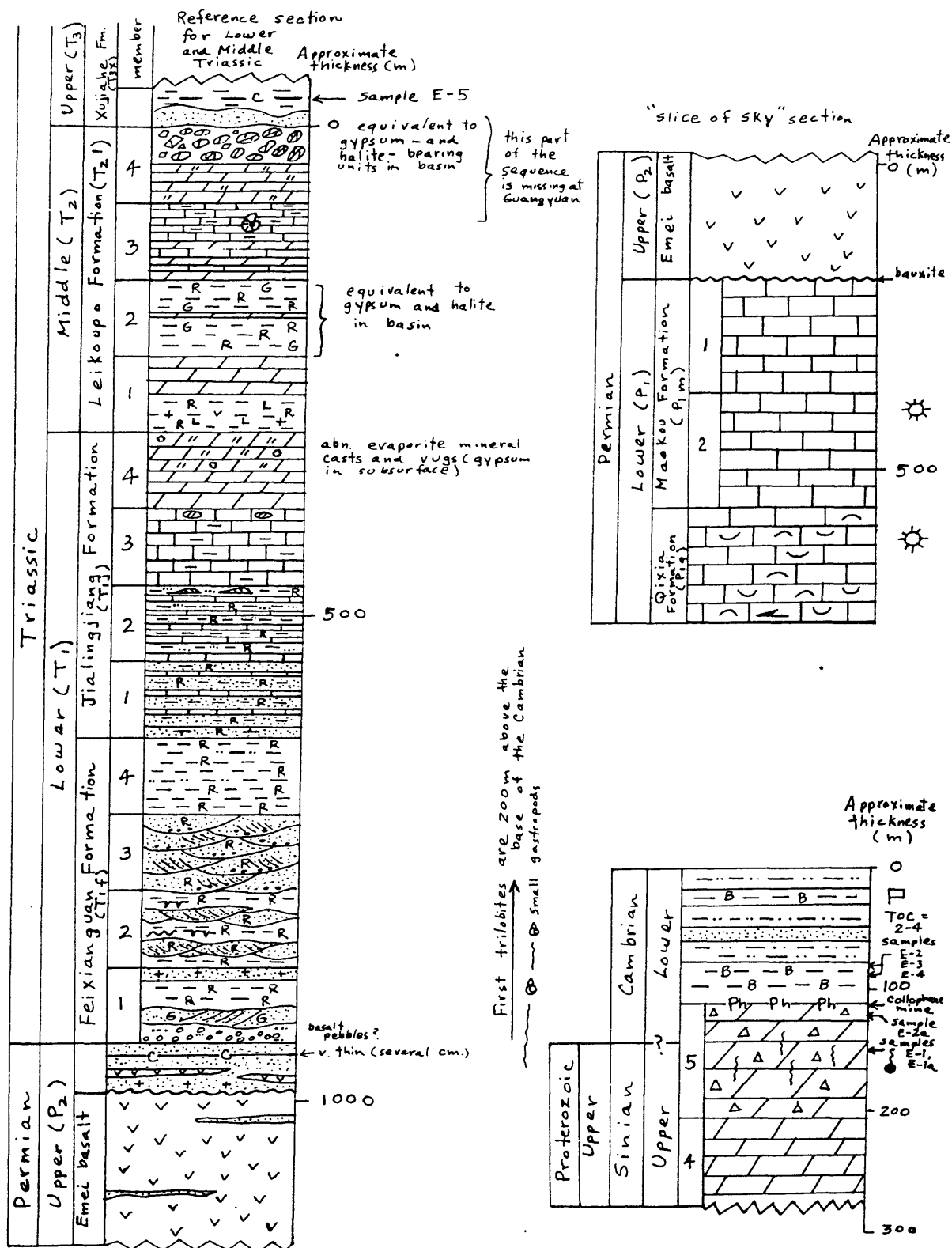
Figure 18. Generalized stratigraphic section of parts of the Sinian, Cambrian, Permian, and Triassic sequence, Emeishan area, Sichuan. Described October 16-17, 1991. See Appendix C for explanation.
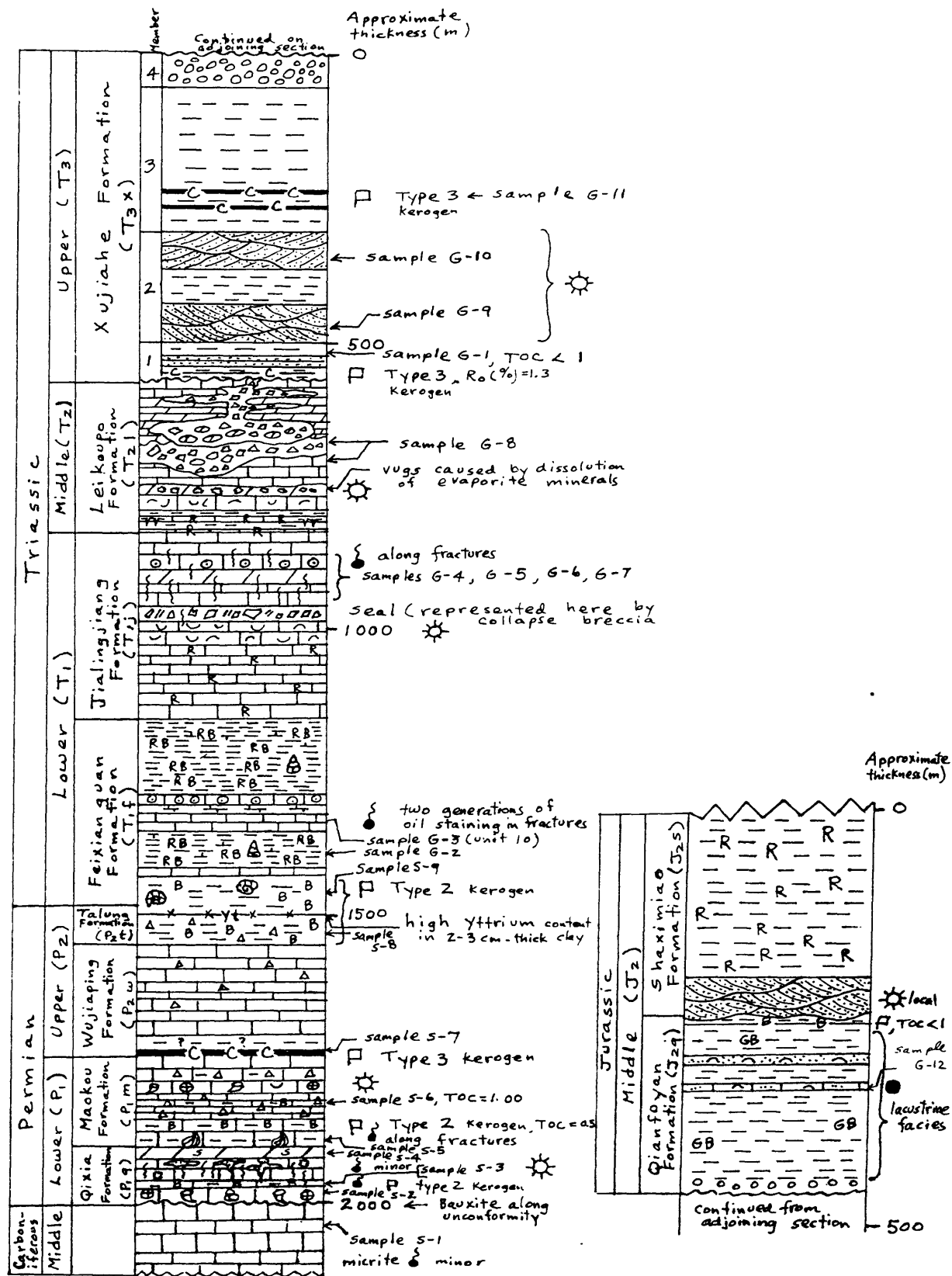
27
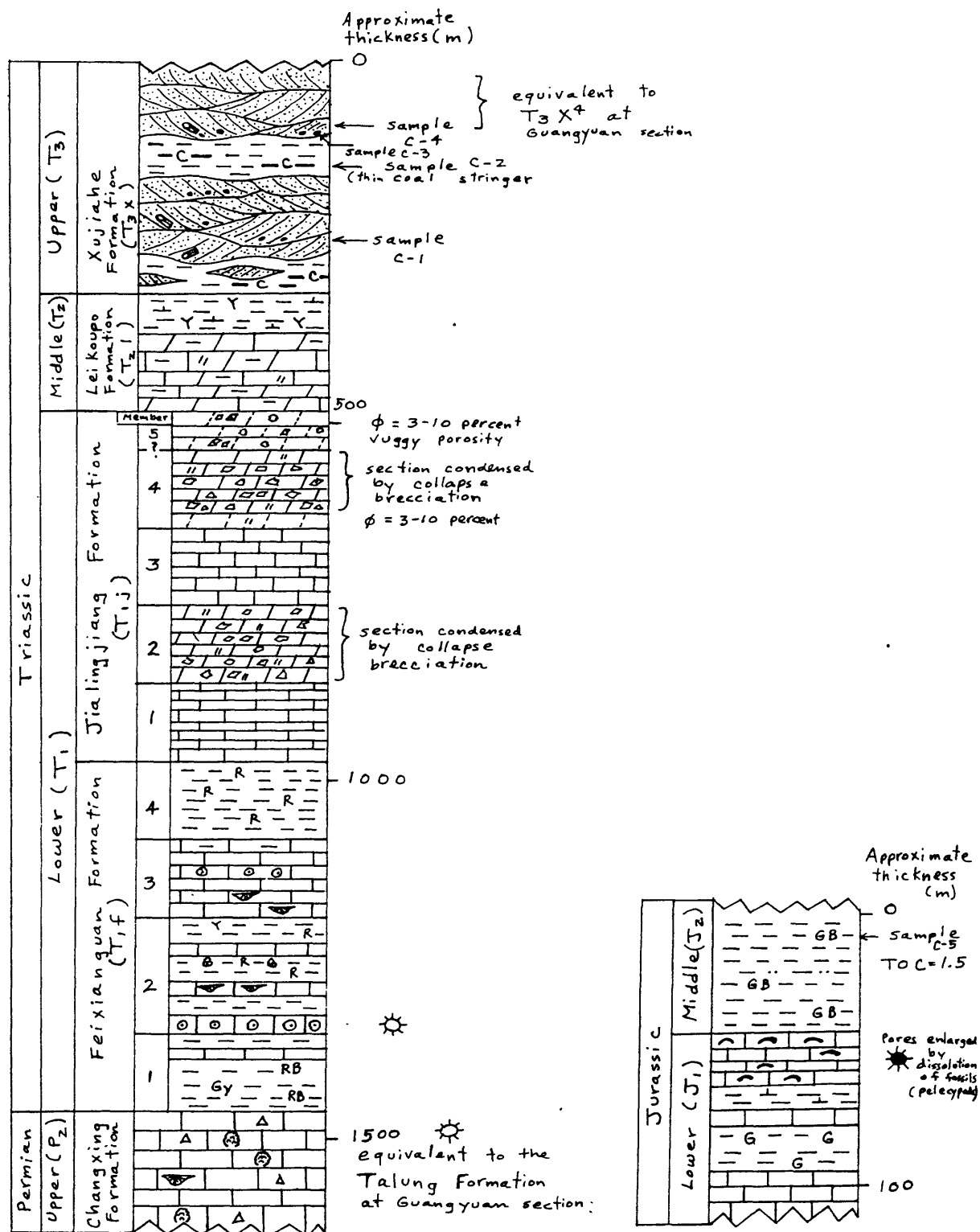
Figure 19. Generalized stratigraphic section of parts of the Permian, Triassic, and Jurassic sequence, Chongqing area, Sichuan. The section is located along the Jialing Jiang near Jiaobashi. Described October 22, 1991. See Appendix C for explanation.

modified extensively by leaching and collapse brecciation. Where available, reservoir character, pressure, and temperature data are supplemented by core observations, lecture notes, and published literature.

Sinian dolomite

Sinian dolomite is the major reservoir unit in the Weiyuan field (fig. 13). In the Emeishan area, outcrops of the Sinian dolomite consist of vuggy and slightly fractured, light gray dolomicrite (fig. 18). Commonly, vugs and fractures are filled with bitumen. The uppermost part of the Sinian dolomite is overlain by a dolomite of Early Cambrian age that is very siliceous and phosphatic. Rice and Ryder sampled vuggy dolomite from core in the Weiyuan No. 28, 110, and 117 wells at 3438 m, 3229 m, and 3016 m, respectively.

According to Madame Liu (presentation at Weiyuan, October 19, 1991), the Sinian reservoir at the Weiyuan gas field was deposited in a tidal flat setting. The best reservoirs consist of carbonate shoal deposits, moderate reservoirs are supratidal and intertidal dolomite, and the poorest reservoirs are subtidal dolomite. The reservoir is highly heterogeneous and consists of intercrystalline porosity, vuggy porosity caused by dissolution and karst processes, and fracture porosity caused by extensional and strike-slip faulting. Locally, wells have drilled into caverns. Porosity in the Sinian dolomite ranges from less than 1 percent to 6 percent and the mean porosity is 2 percent. The mean permeability of the dolomite reservoir is 0.01 millidarcys. Additional evidence of reservoir heterogeneity in the field is the complicated interlayering of water and gas without a well-defined gas-water contact.

The Sinian dolomite reservoir at the Weiyuan gas field has a normal pressure of 295 bars at 3,000 m (0.44 psi/ft gradient) (Madame Liu, presentation at Weiyuan, October 19, 1991).

Carboniferous carbonate rocks

Carboniferous carbonate reservoirs are the most important gas producers in the anticlinal fields of the eastern part of the southeastern fold belt. This unit was briefly observed in outcrop in the Guangyuan area where it consists of gray micrite (fig. 16). Local fractures in the limestone contain bitumen. In southeastern fold belt fields, Carboniferous reservoirs consist of tidal flat dolomite that has experienced extensive tectonic fracturing and karstification caused by widespread pre-Permian uplift and erosion (Chen, 1982; Guo, 1991b). Porosity of the fractured, solution-enhanced reservoirs is as high as 16 percent (Guo, 1991b).

29

Permian carbonate rocks

Gas is produced from Permian carbonate reservoirs throughout the southeastern fold belt and the southwestern end of the central platform. The major producers are the Lower Permian Qixia and Maokou Formations and the Upper Permian Changxing Formation. In the Guangyuan area, the lower one-fourth of the Qixia Formation consists of micrite, biomicrite, and biosparite with whole fossils and fragments of crinoids, coral, and pelecypods (fig. 16). The upper three-fourths of the Qixia Formation consists of a shoaling-upward sequence with black to dark brown argillaceous micrite at the base, white micrite with dissolution vugs and solution cavities in the middle, and coarsely crystalline dolomite of supratidal origin at the top (fig. 16). The dark argillaceous micrite at the base of the shoaling-upward sequence contains oil in local vugs. Bitumen-filled fractures are also noted in the Qixia Formation in the Guanxian area (fig. 17).

A basal micrite containing large productid brachiopods and oil-filled fractures marks the base of the Maokou Formation in the Guangyuan area (fig. 16). The remainder of the Maokou Formation consists of two upward-shoaling sequences that grade from black to brown argillaceous, cherty limestone at the base to micrite, biomicrite, and biosparite at the top. Fossil constituents are coral, crinoids and pelecypods. Both the Qixia and Maokou Formations produce gas in the Ziliujing field (fig. 9).

The Upper Permian Changxing Formation in the Chongqing area is characterized by dark gray biomicrite with local sponge bioherms, brachiopods, and chert nodules (fig. 19). This formation is equivalent to the Talung Formation of deep water origin in the Guangyuan area. Liu and others (1991) have described in detail several types of gas-producing carbonate buildups in the Changxing Formation. Dolomitization is most extensive in the platform-margin reefs and these contain the best gas reservoirs (Liu and others, 1991). Vuggy dolomite cored at 3,231 m in the Jiannan No. 34 well, Jiannan gas field (fig. 2) probably represents a dolomitized reef in the Changxing Formation. Rice and Ryder collected a sample of this core.

Lower and Middle Triassic carbonate rocks

Lower and Middle Triassic carbonates are important and widespread gas reservoirs in the Sichuan basin (figs. 8,9,10). The major gas producers are the Lower Triassic Feixianguan and Jialingjiang Formations and the Middle Triassic Leikoupo Formation. These formations produce gas throughout the southeastern fold belt and the southwestern end of the central platform. Nearly complete sections of the Lower through Middle Triassic sequence crop out in the Guangyuan, Emeishan, and Chongqing areas (figs. 16,18,19).

The Lower Triassic Feixianguan Formation consists primarily of thin-bedded, calcareous, locally fossiliferous, red-brown mudstone and shale and light gray fossiliferous micrite and oosparite. Marine limestone beds are most common in the Guangyuan and Chongqing sections (figs. 16,19). In the Emeishan section the Feixianguan Formation is nonmarine and consists of fluvial sandstone interbedded with red mudstone and siltstone (fig. 18). The basal 50 m of the Feixianguan Formation in the Guangyuan section is marked by an ammonite-bearing, black calcareous shale that grades upward from the siliceous black shale of the Upper Permian Talung Formation (fig. 16). Also in the Guangyuan area, a 50- to 60-m-thick micritic limestone near the middle of formation has local oil-filled fractures. Oolitic limestones (oosparite), such as those observed in the Changqing area, are considered to be the best gas reservoirs in the Feixianguan Formation. Vuggy dolomite in the Feixianguan Formation, cored at 2929.5 m, in the Jiannan No. 28 well, is an important reservoir in the Jiannan field (fig. 3). This core was sampled by Rice and Ryder.

Shallow marine limestone, tidal flat dolomite, and sabkha? evaporites constitute the Lower Triassic Jialingjiang Formation (fig. 16, 18, 19). The highest quality reservoirs are grainstone (biosparite), oolitic limestone (oosparite), vuggy dolomite, and dedolomite with intercrystalline porosity. Carbonate dissolution has enlarged pore space and karst-induced fractures in the Jialingjiang reservoirs during extended periods of subaerial exposure of the shelf and tidal flat. However, the influence of dissolution is difficult to recognize in outcrop because of the disrupted bedding caused by Holocene leaching and collapse brecciation (figs. 16,19). Tectonic fractures have enhanced the porosity and permeability of the Jialingjiang reservoirs as shown by the oil-bearing open fractures in the Guangyuan area (fig. 16). The porosity of the bioclastic and oolitic reservoirs is as high as 9 percent and permeability ranges from 1 to 10 md (Guo, 1991b).

The Middle Triassic Leikoupo Formation is similar to the Jialingjiang Formation except the Leikoupo Formation contains a higher percentage of red shale, dolomite, and evaporite beds (figs. 16,18,19). The major reservoirs are bioclastic limestone (grainstone) and vuggy dolomite whose vugs were produced by evaporite-mineral dissolution (fig. 16). As in the Jialingjiang Formation, many details of the reservoir character of the Leikoupo Formation are obscured in outcrop by evaporite leaching and collapse brecciation during the Holocene. Part of the gas at the Wolonghe and Zhongba fields is produced from dolomite of the Leikoupo Formation (figs. 10,12).

Upper Triassic sandstone

Sandstone reservoirs in the Upper Triassic Xujiahe Formation produce gas at the Zhongba field (fig. 12) and at the unnamed tight-sandstone gas field near Deyang (fig. 3). The Xujiahe Formation is

predominantly nonmarine in origin and consists of fluvial sandstone, carbonaceous gray shale, coal, siltstone, and conglomerate (figs. 16,17,19). Member 2 of the Xujiahe Formation, the main gas reservoir, is characterized by composite, medium-to large-scale crossbedded fluvial sandstone bodies that commonly are 50 to 100 m thick (figs. 16,17). The sandstone beds are fine to medium grained but commonly are coarse grained. Abundant clay clasts and wood fragments are usually located near the base of each channel-form unit.

Quartz, lithic fragments and feldspar are the main mineral constituents of the framework grains. At Guangyuan the sandstones appear to be quartzose and reasonable free of lithic fragments and argillaceous matrix, whereas at Guanxian the sandstones contain less quartz and higher quantities of lithic fragments, feldspar, and argillaceous matrix (figs. 16,17). Guo (1991b) reports that lithic fragments in the Xujiahe Formation commonly exceed 20 percent.

The porosity of the Xujiahe Formation ranges between about 2 and 6 percent, whereas the permeability ranges between 0.01 and about 2 md (Guo, 1991b). Secondary intergranular porosity caused by the dissolution of unstable lithic fragments and feldspar is the most common porosity type. Tectonic fractures provide fracture porosity and increased permeability for the sandstone reservoirs (Guo, 1991b).

Reservoir pressure at the unnamed tight-sandstone gas field near Deyang range from 1.8 to 2.0 times normal hydrostatic pressure (0.79-0.88 psi/ft) indicating relatively recent gas generation (Guo Zhengwu presentation at Chengdu, October 7, 1991). The temperature of the Upper Triassic sequence ranges from 100 to 160°C in the northwestern depression (Guo, 1991b).

Jurassic limestone and sandstone

Bioclastic limestone (packstone and grainstone) of lacustrine origin is the most common oil reservoir in the Sichuan basin. The highest quality reservoirs seem to occur where bioclastic limestone was exposed to subaerial conditions during local or regional uplift and leached by circulating ground water (Yin, 1985). Intergranular porosity of the bioclastic limestone reservoirs ranges from 1 to 7 percent. Fracture porosity may be important locally. Lower Jurassic bioclastic limestone crops out in the Chongqing area as a 30-m thick, shoaling-upward sequence bound by green to green brown mudstone (fig. 19). The grainstone beds here have pore space that probably has been enlarged by dissolution processes. Thin, nonreservoir, bioclastic limestone beds of the Middle Jurassic Qianfoya Formation, that are equivalent to oil reservoirs in the central uplift, crop out in the Guangyuan area (fig. 16).

A 50- to 100-m-thick, basal fluvial sandstone unit of the Middle Jurassic Shaqimiao Formation crops out in the Guangyuan area (fig.

32

16). Gas is locally produced from this sandstone in the northwest depression.

TRAPS AND SEALS

Tightly compressed, faulted anticlines--many of which have surface expression--are the most important traps for nonassociated gas in the Sichuan basin. Multiple zones of bedding plane detachment and multiple reservoirs are characteristic of many of these structural traps (Zhai and others, 1987). Not all anticlines are gas productive (fig. 3). A reasonable explanation is that gas was originally present in the barren structures, but due to multiple phases of intense deformation, it has escaped through numerous structurally induced conduits. A second factor may be that gas has been bypassed in the first round of drilling because of structural complications. Disharmonic folding, commonly with multiple levels of detachment having different closures, requires the use of modern seismic profiles to accurately define traps (Bally and others, 1986; China Oil, 1987b).

Oil in Jurassic reservoirs is trapped in open, unfaulted anticlines on the central uplift (fig. 3). As is the case for the tight anticlinal traps, not all of the anticlines are productive. Here, the distribution of oil-bearing structures seems to be controlled by the availability of lacustrine source beds and reservoirs (Yin Jiantang, presentation in Chengdu, October 7, 1991).

Stratigraphically trapped oil and(or) gas accumulations are recognized in two fields: 1) the Guehua oil field (figs. 3, 15) that involves updip permeability changes in Jurassic reservoirs across a structural terrace and 2) part of the Jiannan gas field (fig. 3) where an Upper Permian patch reef has trapped gas on the northeast-plunging nose of the Jiannan anticline (Liu and others, 1991). Potential regional truncation traps along the east side of the central uplift, where Silurian and Carboniferous strata subcrop and extensive dissolution of Cambrian and Ordovician strata has occurred beneath the Permian unconformity, have so far proven to be unproductive (Bao and others, 1985; Guo Zhengwu, presentation in Chengdu, October 7, 1991). Potentially large stratigraphic traps created by regional unconformities also provide drilling targets along the west side of the central uplift.

Evaporite beds in the Lower and Middle Triassic sequence are excellent seals. The thickest evaporite beds probably coincide with depocenters in the northern and northeastern parts of the basin where 2200 to 3000 m of Lower and Middle Triassic strata accumulated (Bao and others, 1985). Remnants of evaporite-bearing strata at widely separated outcrop localities such as Guangyuan, Emeishan, and Chongqing (figs. 16,18,19) suggest that the evaporite beds are regional seals. Red shale and mudstone of the Lower Triassic Feixianguan Formation constitute another seal with basinwide dimensions (figs. 16,18,19). Good seals of more local extent are

33

provided by Cambrian and Silurian shale beds as thick as 500 m (Korsch and others, 1991). Given the intense deformation of the basin, the abundant gas that remains trapped is attributed here, largely, to the effectiveness of these evaporite and shale seals.

SOURCE BEDS, THERMAL MATURATION, AND MIGRATION

Stratigraphic Position and Organic Richness of Source Beds

Paleozoic and Mesozoic source beds have been identified in the Sichuan basin and many of them are available for study in outcrop and(or) selected cores. Moreover, scattered analyses of source-bed richness, expressed as total organic carbon content (TOC), are available in published and unpublished reports. Core and outcrop samples collected by Rice and Ryder are identified in this report but analyses have not been completed. Proposed source beds of questionable quality are omitted in this discussion. For example, Sinian dolomite is dismissed as a significant source bed because its TOC values range from 0.04 to 0.5% and average <0.1% (Korsch and others, 1991).

Lower Cambrian black shales are the oldest known source beds in the basin. These shale beds are distributed throughout the basin but are thickest and most organic rich around the southern and eastern perimeter of the central uplift. Very likely, Lower Cambrian black shale is the major source of natural gas in the giant Weiyuan gas field. Samples of the Lower Cambrian black shale were collected by Rice and Ryder at the Weiyuan gas field from 2,556 m and 2,781 m in the Weiyuan No. 106 well and from 2,875 m in the Weiyuan No. 4(?) well. Here, the Cambrian sequence is about 800 m thick of which the black shale sequence constitutes approximately the lower 300 m. Lower Cambrian black shale crops out in the Emeishan area but it is less than 20 m thick (fig. 18). TOC values from the Weiyuan field and Emeishan area are reported to range from 2 to 4%. Cambrian shale from two unidentified localities in the Sichuan basin contain type I kerogen and have average TOC values of 0.4 and 0.45% (data from the Southwest Bureau of Petroleum Geology reported in Korsch and others, 1991).

Between 300 and 600 m of Lower Cambrian black shale, oil prone and with TOC values commonly between 1 and 5%, were deposited in a deep-water marginal sea at the southeast margin of the Yangtze platform (fig. 20). As we will discuss later in this section, Lower Cambrian black shale now located in the southern part of the central uplift, southeastern fold belt, and the eastern part of the Qiyaoshan fold belt is a major source for natural gas in the Sichuan basin.

Silurian black shale is considered to be another important oil-prone source bed in the Sichuan basin. It may have supplemented Lower Cambrian black shale as the source of natural gas in the Weiyuan gas field. The Silurian source-bed interval attains a thickness of 400 to 600 m along the southeast margin of the Yangtze

34

platform (fig. 20) and thins westward to a zero edge at the eastern and southwestern-most margins of the central uplift. Silurian strata are absent in the Emeishan area (Liu, 1988) but are present on the flanks of the Weiyuan gas field where they are about 50 m thick. East of Weiyuan, between Zigong and Luzhou, Silurian shale beds are 600 to 700 m thick (Korsch and others, 1991). Two samples of Silurian black shale were collected by Rice and Ryder between 1568 and 1576 m in the Weiyuan No. 106 well. Silurian shale from two unidentified localities in the Sichuan basin contain type I kerogen and have average TOC values of 0.40 and 0.42% (data from the Southwest Bureau of Petroleum Geology reported in Korsch and others, 1991). Chen and Chen (1982) report that four samples from Silurian shale and limestone in the Sichuan basin range from 0.1 to 0.8% and average 0.4%. TOC values from Silurian black shale deposited in the deeper water at the southeast margin of the Yangtze platform are reported to average about 1%.

Oil-prone black limestone and shale source beds of Permian and earliest Triassic age were deposited in a deep-water, intraplatform trough that trends west to west-northwest across the northern margin of the Sichuan basin (fig. 21). These black limestone and shale beds are an important source of natural gas in fields of the southeastern fold belt. In the Guangyuan area, black, argillaceous limestone crops out near the base of the Lower Permian Qixia and Maokou Formations and siliceous black shale crops out as the Upper Permian Talong Formation (fig. 16). Also at Guangyuan, oil-prone source beds crop out as black, ammonite-bearing shale of the lowermost part of the Lower Triassic Feixianguan Formation that has a transitional contact with the underlying Talung Formation (fig. 16). The Permian-Triassic boundary at this locality is situated several meters above a 2- to 3-cm-thick yttrium-bearing clay bed. Rice and Ryder collected samples of black argillaceous limestone from the Qixia and Maokou Formations in the Guangyuan area, several of which contain live oil in vugs and fractures, and of black shale from the lower part of the Feixianguan Formation. The deep-water trough also passes through the area of the Jiannan gas field, in the northeast Sichuan basin (fig. 3), where black limestone of the Maokou Formation and black shale of the Loping Series (Talung Formation) were collected by Rice and Ryder from drill core. The black limestone was sampled at 3920 m in the Jiannan No. 38 well and the black shale sample was taken at 3430 m in the Jiannan No. 39 well. TOC values of the Permian source beds are reported to range between about 0.5 and 5%.

The youngest oil-prone source beds in the Sichuan basin occur in a dark brown to black lacustrine shale sequence of Early and Middle Jurassic age. These rocks, characterized by type II kerogen and deposited in a deep water basinal lacustrine setting, are the source of oil and associated gas in Jurassic reservoirs. The lacustrine depocenter was located in the north-central part of the basin in Early and early Middle Jurassic time and shifted to the east-central part of the basin in late Middle Jurassic time (Yin, 1985). Approximately 300 m of source beds were deposited in the north-
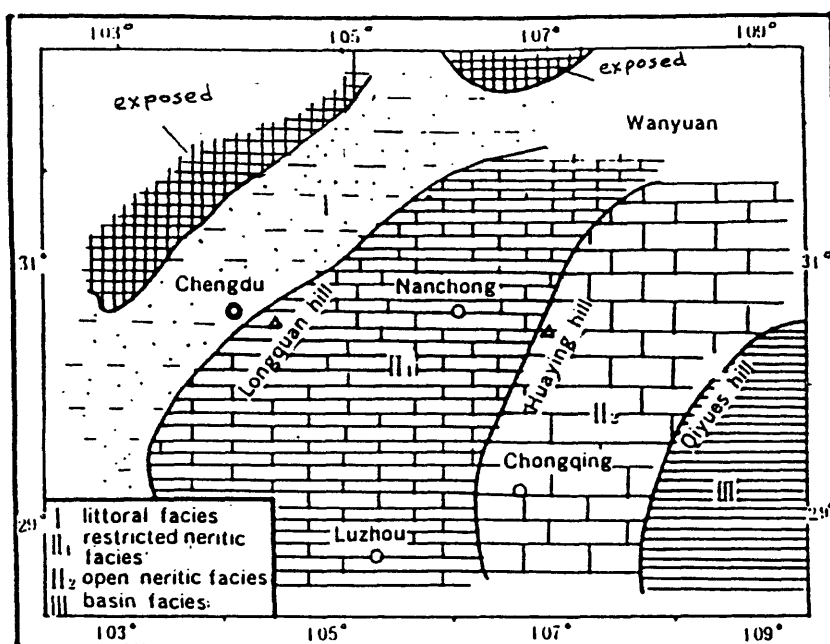
Figure 20. Generalized lithofacies and paleogeographic
map of the Sichuan basin from Late Sinian
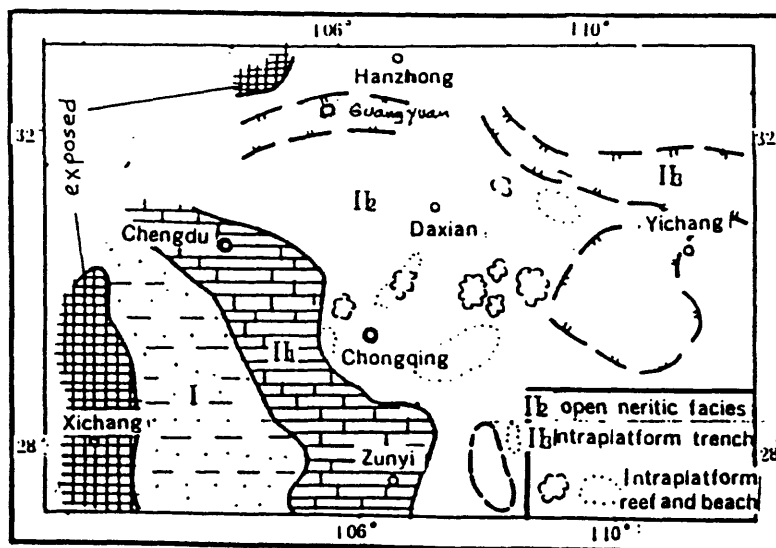through Silurian time (Wang and others, 1989).

Figure 21. Generalized lithofacies and paleogeographic
map of the Sichuan basin during Late Permian
time (Wang and others, 1989). See figure 20
for part of the explanation.

36

central depocenter whereas about 1000 m of source beds were deposited
in the east-central depocenter. The organic-rich lacustrine shale is
confined to the subsurface except where it crops out on the flanks of
the basin as thin beds intercalated with nearshore lacustrine and
fluvial deposits. For example, in the Guangyuan area, a 1- to 2-m
thick black shale crops out at the top of the Middle Jurassic
Qianfoya Formation (fig. 16). This shale bed, reported to have a TOC
value between 0.5 and 1.0%, connects basinward with organic-rich
shale of the north-central lacustrine depocenter. Greenish-brown
lacustrine shale near the margin of the east-central depocenter is
exposed in the Chongqing area (fig. 19). These shale beds do not
appear to be very organic rich but are reported to have TOC values as
high as 1.5%. One sample of the lacustrine shale was collected by
Rice and Ryder at the Chongqing locality (fig. 19).

Gas-prone coal beds at the base of the Upper Permian Wujiaping
Formation and in members 1 and 3 of the Upper Triassic Xujiahe
Formation are important sources of gas in the Sichuan basin. Coal
beds in the Wujiaping Formation are the source and reservoir for much
of the basin's coalbed gas, particularly in mining areas south of
Chongqing, whereas coal beds and carbonaceous shale in the Xujiahe
Formation are the source of gas for Upper Triassic tight sandstone
reservoirs. Moreover, coal beds in the Wujiaping and Xujiahe
Formations may be a secondary source of natural gas for gas fields of
the southeastern fold belt and the adjoining southwestern part of the
central uplift. Coal zones in the Wujiaping Formation and member 3
of the Xujiahe Formation are distributed across most of the Sichuan
basin. In the Guangyuan area, a major 2-m thick coal bed is being
mined in the basal Wujiaping Formation and at least two coal beds, as
thick as 1 m, are being mined in member 3 of the Xujiahe Formation
(fig. 16). Approximately 8 coal beds are being mined in member 3 of
the Xujiahe Formation in the Guanxian area (fig. 17) but several of
them may have been repeated by thrust faults. In the vicinity of
Zigong and the Weiyuan gas field (fig. 3), coal beds are being mined
from members 1 and 3 of the Xujiahe Formation. The coal-bearing
interval in Wujiaping Formation near Chongqing is about 150 m thick
and the coal beds are 1 to 2 m thick. Xujiahe Formation coal beds
are reported to be mined in the Chongqing area but only 1 cm-thick
coal beds were observed in outcrop (fig. 19). Seven samples of coal
and carbonaceous shale were collected by Rice and Ryder at the
previously described outcrop localities (fig. 16-19).

Thermal Maturation

The top and base of the oil window, based on vitrinite
reflectance data, occur at depths of about 1 km and 3 km,
respectively, in the northwestern depression of the Sichuan basin
(fig. 22) (Feng Fukai, presentation in Beijing, October 5, 1991).
Guo (1991b) reports that the maximum depth of oil accumulations is
about 3800 m. From the northwestern depression, the oil window rises
gently southeastward so that it intersects the surface along a wide
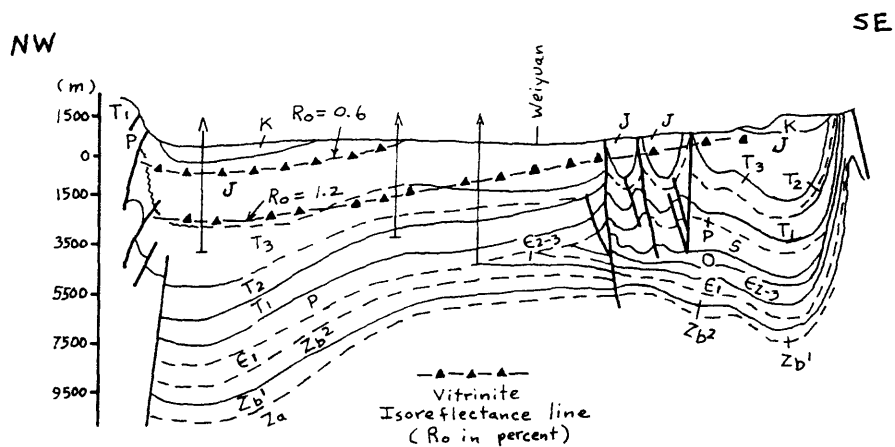belt that crosses the southeastern fold belt and part of the

Figure 22. Generalized cross section through the Sichuan
basin (Sun and others, 1991) showing the
approximate location of vitrinite isoreflectance
lines (Feng Fukai, talk presented in Beijing,
October 5, 1991.

38

adjoining central platform (fig. 22). Vitrinite reflectance values in the Nuji well, Longnusi field (table 2) support this interpretation. Although not shown on figure 22, the oil window and perhaps the gas window, are exposed in frontal thrust sheets along the northwestern margin of the basin.

The generalized locations of the R_0=0.6 percent and R_0=1.2 percent vitrinite isoreflectance lines shown in figure 22 agree with the known distribution of oil and gas fields in the basin whereby oil is largely confined to the Jurassic sequence and gas is largely confined to the Sinian, Paleozoic, and Triassic sequences. A plot of several hundred R_0 values against stratigraphic interval also indicates that oil is most likely to occur in units of Jurassic age and that gas is most likely to occur in units of Sinian through Triassic age (fig. 23). The large number of R_0 values between 0.6 and 1.2 percent for the Upper Triassic rocks indicates that in some localities the oil window extends stratigraphically below the Jurassic sequence (fig. 23). Figure 22 shows that Cretaceous strata in the northwestern depression are immature with respect to oil and gas maturation. Assuming a normal geothermal gradient of 25° to 30°C/km, the shallow depth of the oil window in the northwestern depression and its exposure in the southeastern fold belt suggests at least 2 km of post-maturation uplift and erosion of the basin. Sun and others (1991) and Feng Fukai (presentation in Beijing, October 5, 1991) suggest that this post-maturation uplift and erosion has occurred in the past 10 million years.

Thermal maturation indices for the coal zone at the base of the Upper Permian Wujiaping Formation in the western Yangtze platform, showing R_0 values between 1.5 and 3.5 percent, confirms that the Paleozoic sequence and most of the Triassic sequence are within the gas window (fig. 24). In addition to the expected high maturation indices in the foredeep between Guangyuan and Chengdu, high maturation indices ($R_0 \geq 3.0$ percent) are noted in smaller areas northeast and southwest of Chongqing (fig. 24). The high thermal maturity of the Lower Permian coal zone northeast of Chongqing probably resulted from the Jurassic foredeep in front of the Dabashan fold and thrust belt, whereas the high thermal maturity of the coal zone southwest of Chongqing does not appear to be a burial phenomenon and may represent a heat flow anomaly.

Generation, Migration, and Entrapment

Preliminary subsidence curves and time-temperature plots constructed by Ryder and Rice for the Guangyuan, Guanxian, and Weiyuan localities on the flanks of the basin suggest that the Paleozoic and Triassic source beds entered the oil and gas windows between Silurian and Early Cretaceous time (~400-100 Ma) (figs. 25-27). Jurassic source beds reached the oil window in Late Cretaceous to late Tertiary time (~100-10 Ma). Therefore, oil and gas generation could have taken place from about 400 to 10 Ma, was shut down for awhile about 275 Ma during a period of regional uplift and

39

Stratigraphic interval	Jt^5	Jt^4	Jt^3	Th^6	Th^4	Th^1	Tf^4	P_1^1	ϵ_1^1
Depth (m)	1190	1320	1470	1679	1950	2250	3810	4515	5190
R_o max (%)	1.04	1.11	1.26	1.16	1.31	1.41	1.48	2.97	3.19

Table 2. R_o (in percent) values for selected stratigraphic intervals in the Nuji well, Longnusi field (Zhai and others, 1987). See figures 2, 3, and 29 for the location of the Nuji well.

40
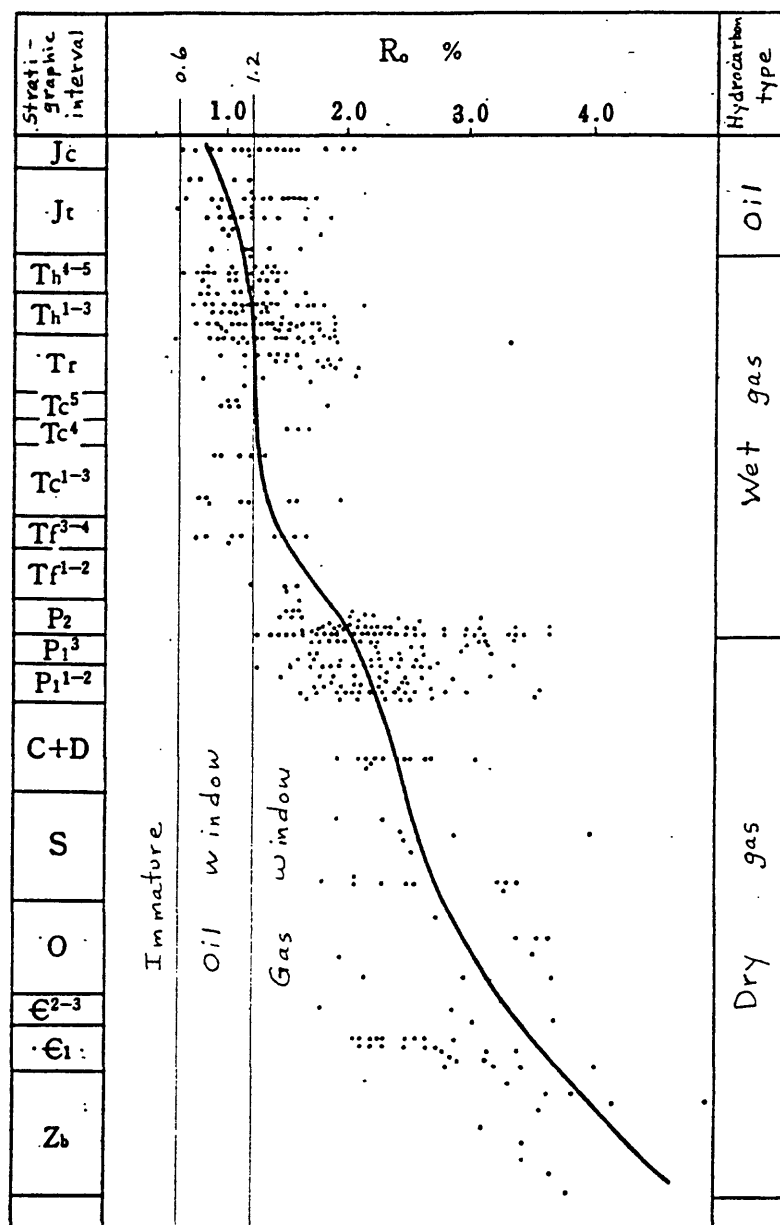
Figure 23. Plot of Ro(in percent) values against stratigraphic interval for the entire Sichuan basin (Zhai and others, 1987).
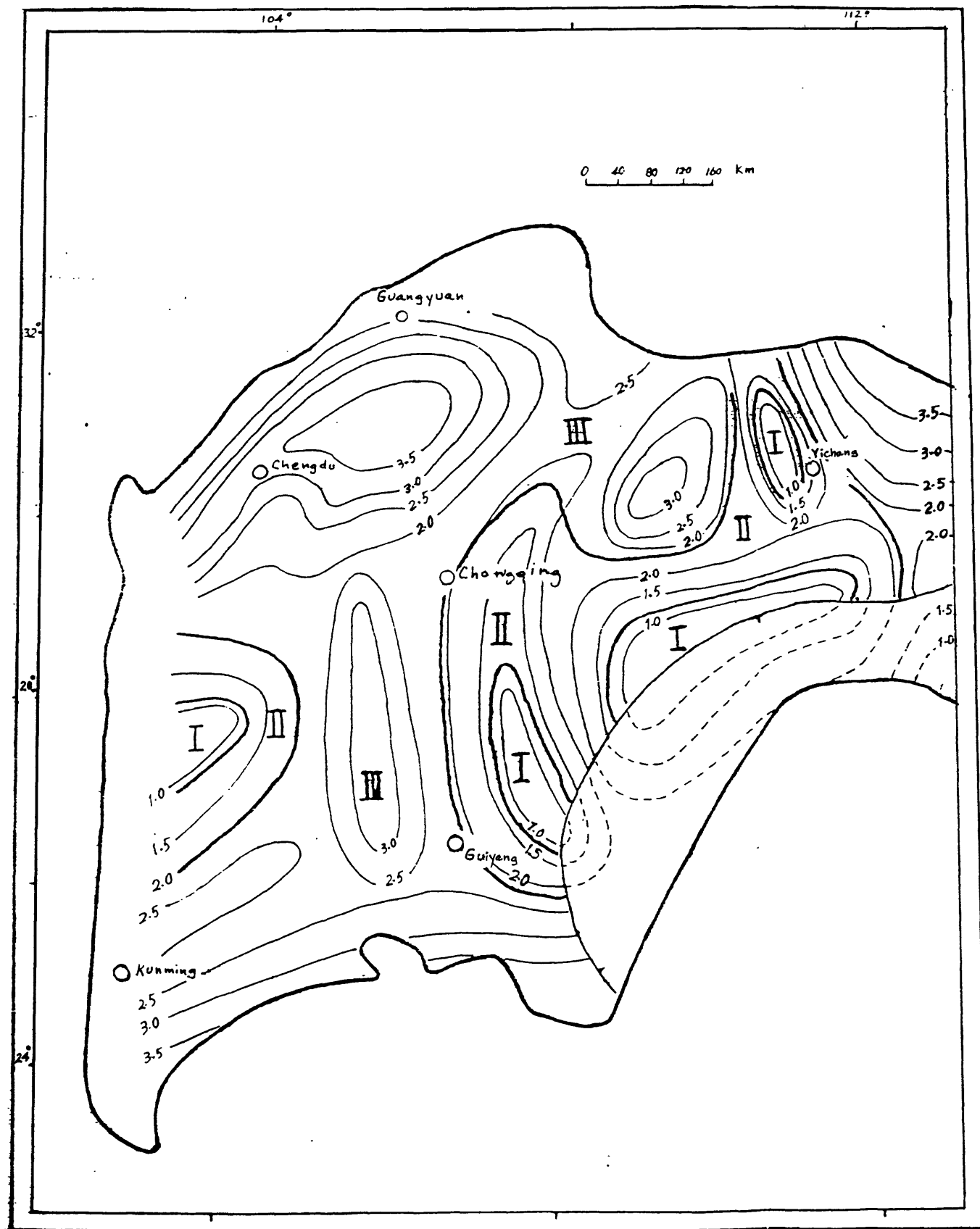
Figure 24. Distribution of Ro(in percent) values for the coal zone
at the base of the Upper Permian Wujiaping Formation
(P_2w), western Yangtze platform.
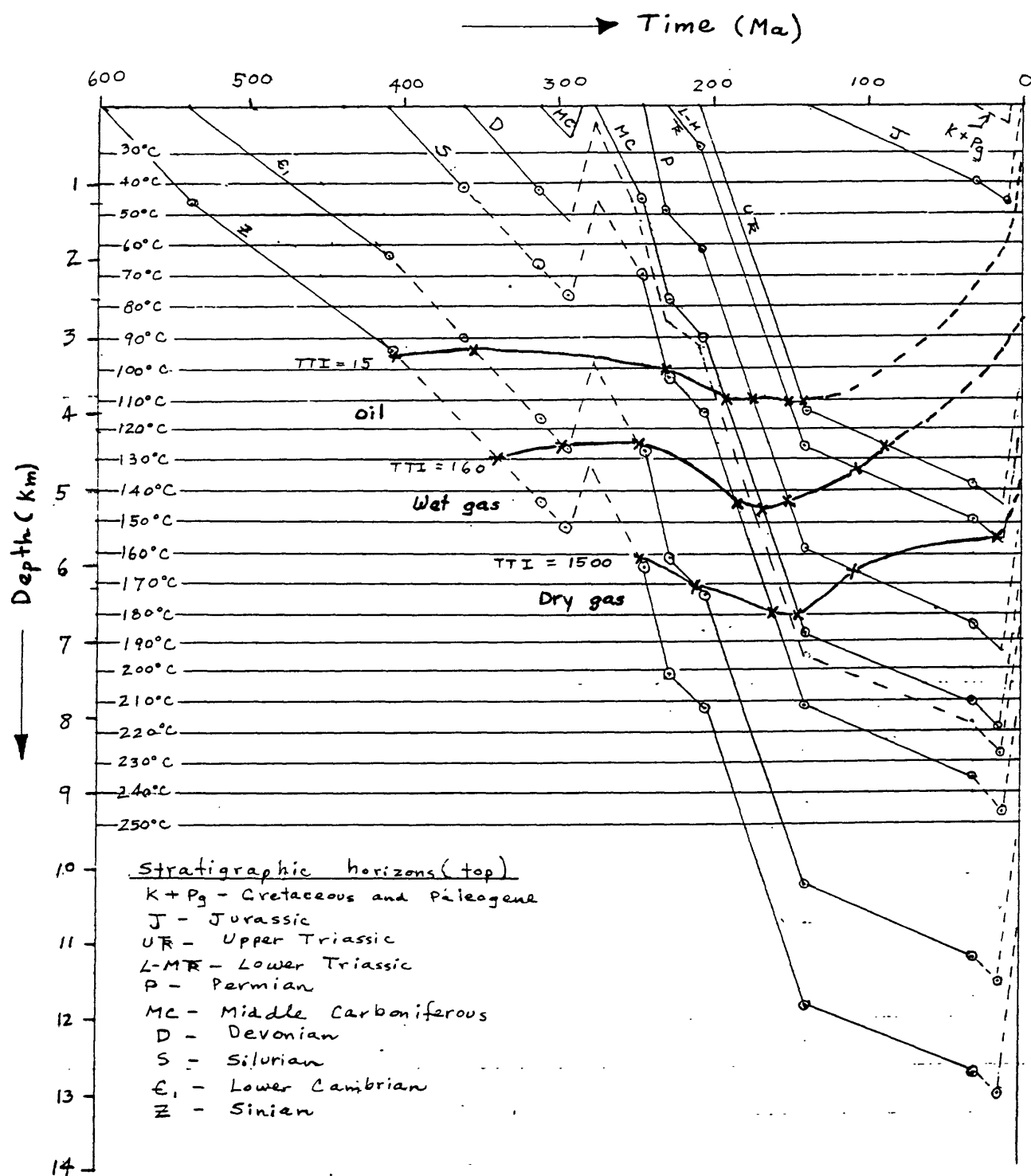
Figure 25. Subsidence history and time-temperature plot for the Guangyuan area, northwestern depression, northern Sichuan basin. Average surface temperature is about 15°C. Geothermal gradient = 25°C/km.
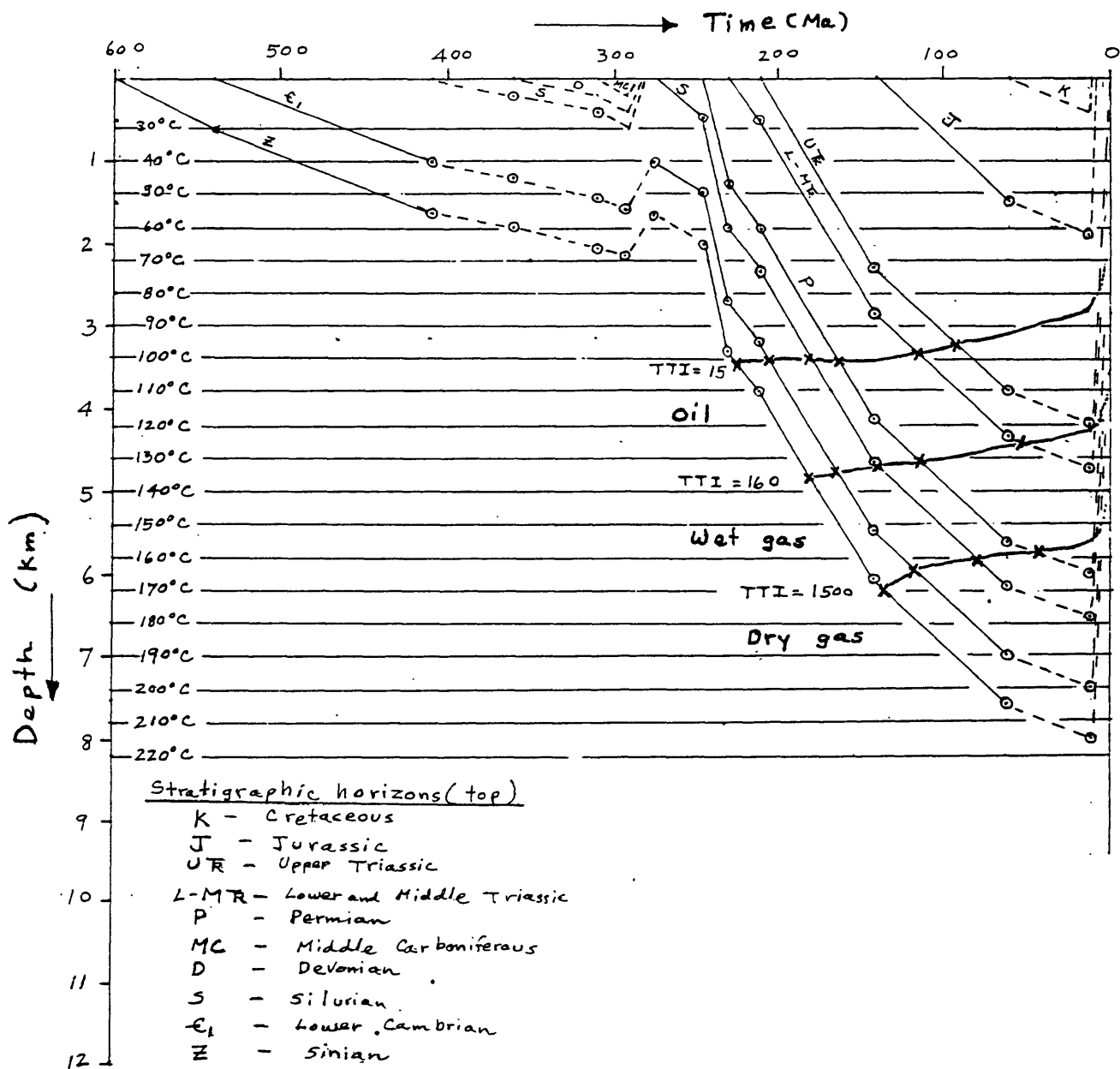
43
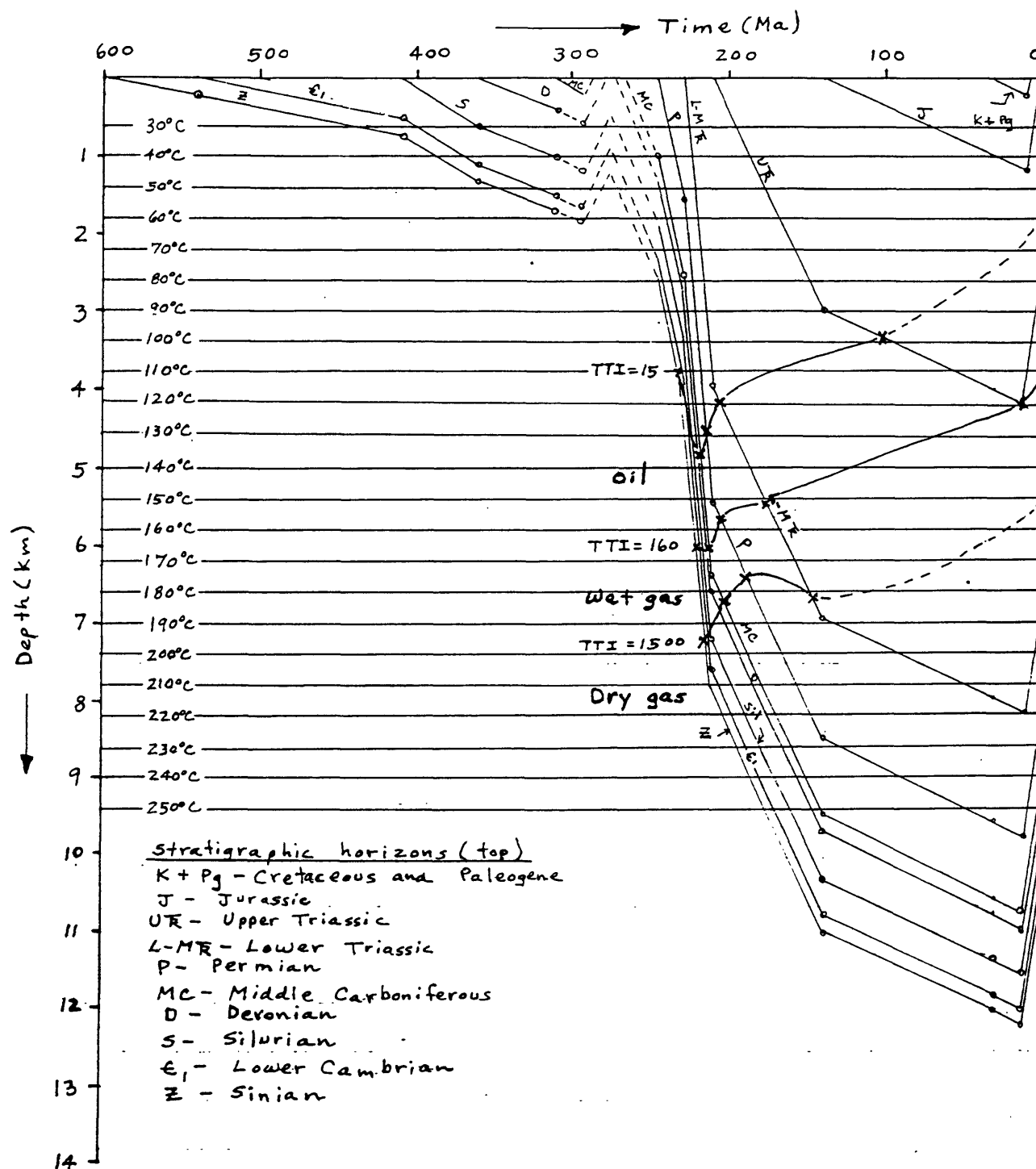
Figure 26. Subsidence history and time-temperature plot for the Guanxian area, northwestern depression, western Sichuan basin. Average surface temperature is about 15°C. Geothermal gradient = 25°C/km.

Figure 27. Subsidence history and time-temperature plot for the Weiyuan area, central uplift, southwestern Sichuan basin. Average surface temperature is about 15°C. Geothermal gradient = 25°C/km.

erosion, and was shut down permanently at about 10 Ma with post-middle Himalayan uplift and erosion. Moreover, most of the gas in the basin, except for gas in tight Upper Triassic sandstone reservoirs and coalbed gas in Permian and Triassic coals, resulted from cracking of oil generated from marine source rocks mostly of Paleozoic age.

Sun and others (1991) propose a complex history of hydrocarbon evolution where major phases of hydrocarbon genesis coincide with orogenic stages in the basin's evolution (fig. 28). They postulate the importance of Caledonian (~400 Ma) and early Indosinian (~230 Ma) long-range oil migration events from outside the basin (fig. 28). This oil is thought to have been generated from Cambrian and Silurian black shale deposits that bordered the southeastern edge of the Yangtze platform and migrated northwestward into the Weiyuan and Guizhou paleohighs (Qiu Yunyu, presentation in Wuxi, October 23, 1991). Giant bitumen (biodegraded oil) accumulations in Silurian, Ordovician and Cambrian strata near Guiyang, Guizhou province (fig. 29), represent at least 7 billion barrels of oil that probably were trapped during Caledonian and early Indosinian migration and exhumed and degraded during late Tertiary uplift and erosion (Sun Zaocai and Qiu Yunyu, oral communication, October 23, 1991).

Early in the Yanshanian phase (~150 Ma), oil that was trapped in paleohighs and truncation traps during episodes of long-range and local migration was thermally decomposed to gas and solid bitumen (fig. 28). Increased burial at this time also produced increasing amounts of thermal gas from local oil-prone Permian and Lower Triassic source beds that had reached the gas window. Later in the Yanshanian phase (~100-65 Ma), thermal gas was generated from gas-prone Permian and Upper Triassic coal beds. According to Sun and others (1991), gas generated during the Yanshanian orogeny was preserved from atmospheric escape by keeping it in solution until the Himalayan orogeny when thin-skinned anticlinal traps became available. Some mixing of the thermal gases was inevitable but, because of very efficient seals, most of the gases were isolated from one another.

Free gas was released from deep subsurface host fluids during Himalayan tectonism (~35-10 Ma) and migrated along multiple pathways provided by Himalayan thrust faults and tectonic fractures (Sun and others, 1991). This migration caused additional mixing of gas, accumulation of gas in tightly compressed, thrust-faulted anticlines, and escape of large amounts of gas to the atmosphere (fig. 28). Post-middle Himalayan (~10 Ma) uplift and erosion exacerbated the escape of gas from the basin and terminated gas generation.

Because of widespread migration, high rates of diffusion, and active tectonism, gas generated in the basin during the Yanshanian orogeny (~150-100 Ma) may have vanished into the atmosphere. Thus, late-stage generation of gas in the basin is a possible alternative to the model proposed by Sun and others (1991). This alternative
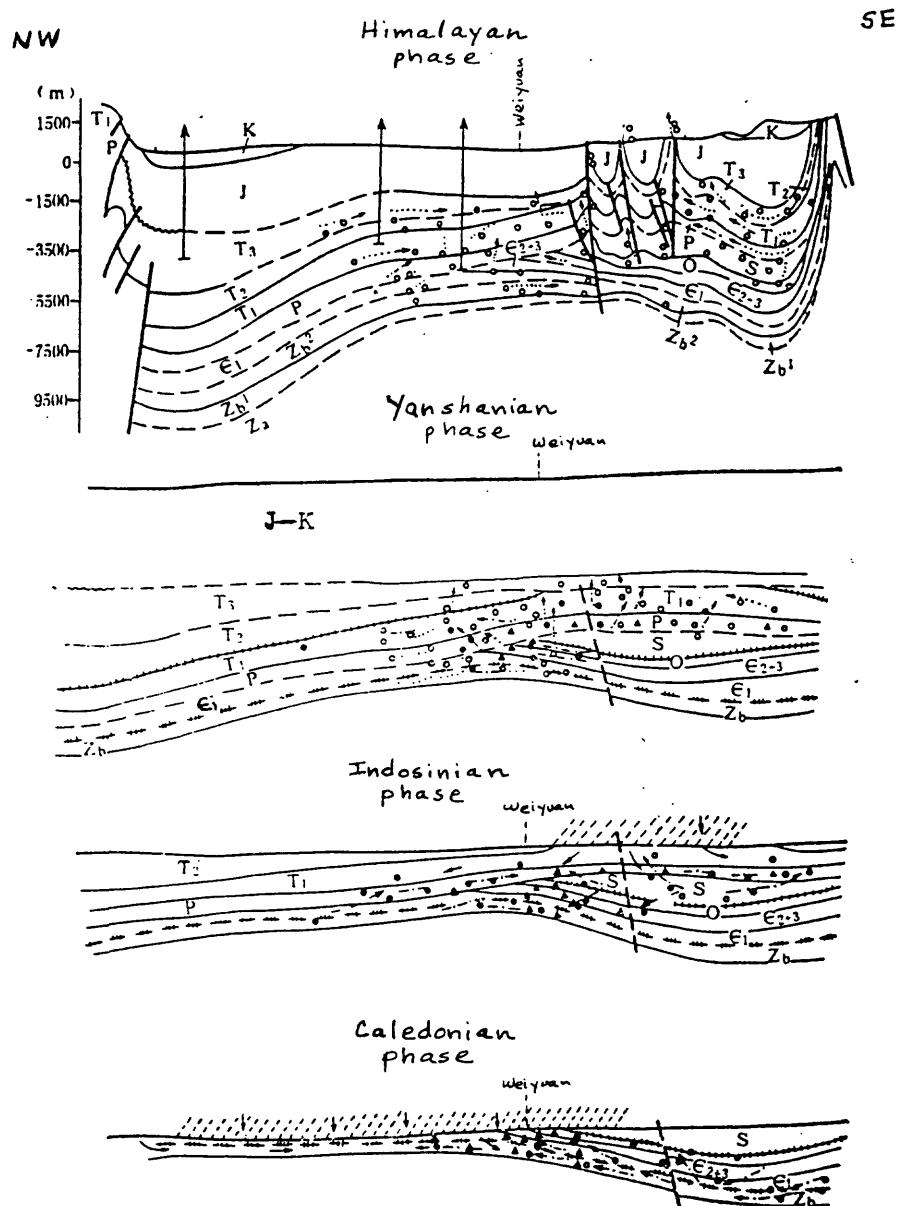
46

Figure 28. Major phases of oil and gas generation and migration
in the Sichuan basin (Sun and others, 1991).
O Gas, ● Oil, ▲ Bitumen, ◄--- Oil migration, ◄— Water,
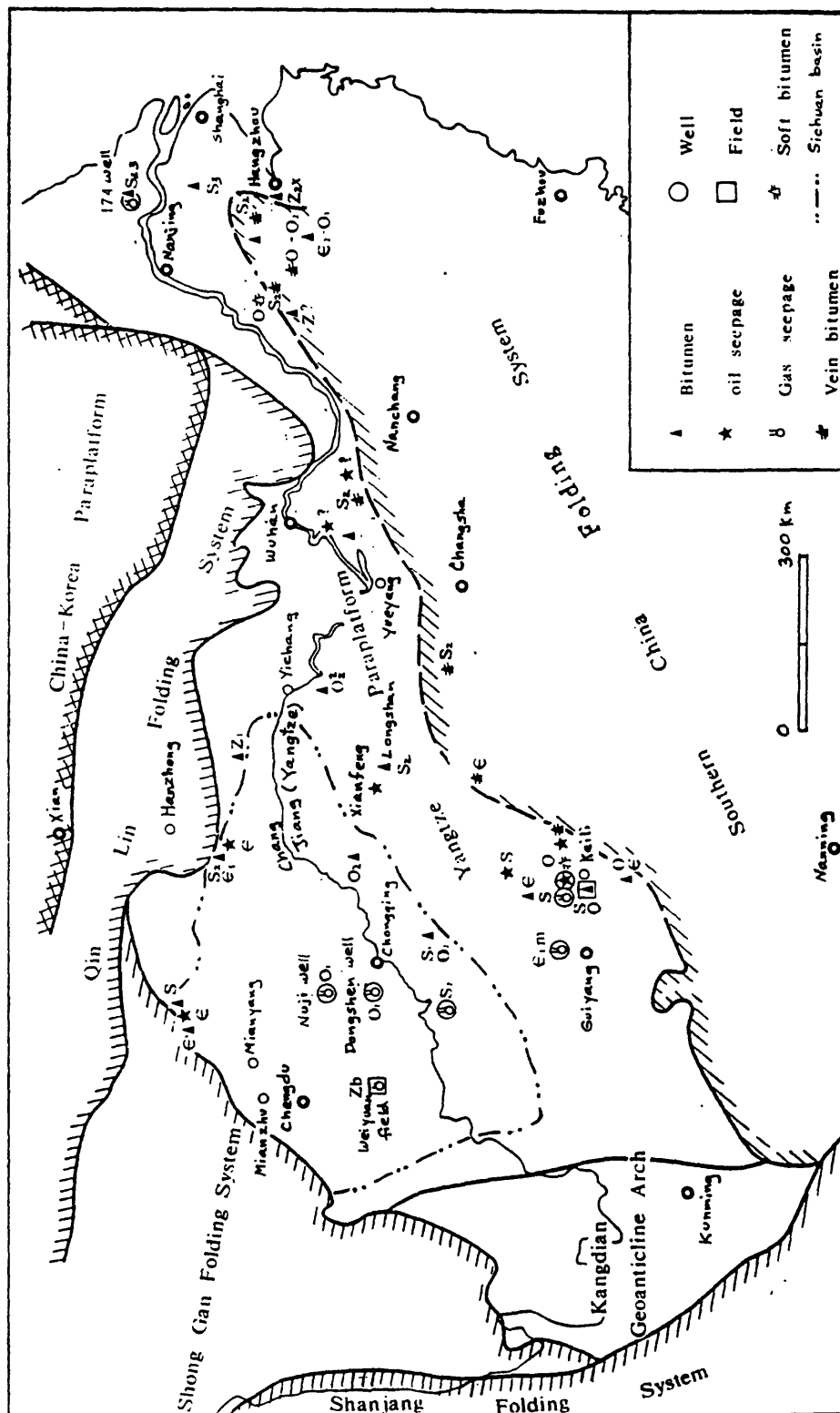◄----- Gas migration, ++++ Disconformity, ///// Subaerial
exposure

Figure 29. Location of selected oil seeps, gas seeps, and bitumen deposits in the Yangtze platform (Qiu, Xu, and others, 1986).

model treats gas generation from cracked oil as a relatively recent phenomenon (20-10 Ma) that occurred during the latest stages of basin subsidence and sedimentation. Gas generation probably was permanently shut down after post-middle Himalayan (~10 Ma) uplift and erosion so that gas presently leaking to the atmosphere is not being replaced by recently generated gas.

Oil was generated from Jurassic oil-prone lacustrine source beds in the late Yanshanian (~80-65 Ma) and early Himalayan (~35-30 Ma) phases. Most of this oil migrated a short distance into lacustrine limestone and sandstone reservoirs where it accumulated in anticlinal and stratigraphic traps on the central uplift. Local gas accumulations in Jurassic reservoirs may have been charged by vertical leakage of gas generated from underlying Upper Triassic coal beds (Guo Zhengwu, presentation in Chengdu, October 7, 1991).

GEOCHEMICAL CHARACTER OF NATURAL GAS

Nonassociated natural gas in the Sichuan basin is composed predominantly of methane and noncombustible gases nitrogen, carbon dioxide, and hydrogen sulphide (tables 3,4,5). The dryness or proportion of methane in the hydrocarbon phase, expressed as C_1/C_1-C_5 values, ranges from 0.92 to 1.00 (tables 3,4), indicates that the gas is dry to very dry. Commonly, C_1/C_1-C_5 values increase with the age of the gas reservoir (table 3). The isotopic composition of the methane in the nonassociated gas ranges from $\delta^{13}C$= -31 to -40 per mil (table 3, fig. 30). In contrast, natural gas associated with Jurassic reservoirs is moderately wet as defined by C_1/C_1-C_5 values between about 0.81 and 0.88 (table 4). Moreover, associated gas tends to have lower amounts of noncombustible gas and lighter isotopic values (methane $\delta^{13}C$= -40 to -47 per mil) than the nonassociated gas (table 4, fig. 30).

Based on molecular and isotopic composition and thermal maturity of associated source rocks, nonassociated natural gas in the Sichuan basin is interpreted to be high-temperature thermogenic resulting from thermal cracking of pre-existing oil and heavier hydrocarbons. By this process, generated oil and heavier hydrocarbons are broken down thermally into successively simpler and more chemically stable products that end with methane (CH_4). Nitrogen, carbon dioxide, and hydrogen sulphide usually constitute a combined total of 3 percent or more of the gas and reflects a continuation of the thermal maturation process whereby mature methane-rich gas is diluted by noncombustible gas. Nitrogen gas probably originated by thermal decomposition of nitrogen compounds or by degassing of the deep crust or mantle. Carbon dioxide gas probably originated by thermal decomposition of carbonates. Thermochemical reduction of sulphate in widespread Triassic anhydrite beds and in less extensive Sinian and Cambrian anhydrite beds is the most likely origin of the hydrogen sulphide gas. The relatively heavy isotopic composition of the hydrocarbon gas suggests a prolonged history of thermogenic reactions. The

Table 3. Geochemical character of natural gas in the Sichuan basin arranged by stratigraphic position of the reservoir unit (Sun and others, 1991).

Period	Geologic Age	C₁	C₂	C₃+	$\frac{C_2}{C_1-C_5}$	Normal	Iso-prenoid	Me—	Mes—	Cyclo	ΣIso	$\frac{C_{10}+C_{11}+C_{12}+C_{13}+C_{14}}{C_{15}+C_{16}+C_{17}+C_{18}}$	Peak carbon number	δ¹³C₁	δ¹³C₂	δ¹³C₂—δ¹³C₁
Triassic	Tc⁵	91.1	0.86	1.81	0.92	15.1	9.1	36.6	31.4	7.0	84.9		nC₂₃	-33.64	-33.19	0.47
	Tc³	96.8	1.19	1.54	0.97	Tℓ²:								—	—	—
	Tc²	96.6	1.53	2.07	0.96	34.6	10.3	33.1	9.2	2.5	65.2	2.6	nC₂₂	-33.78	-32.94	0.87
	Tℓ	96.9	0.89	1.20	0.98	36.2	11.6	30.1	9.7	2.2	63.6	2.0	nC₂₃	-34.57	-33.74	1.27
Permian	P₂¹	98.1	0.84	0.90	0.98									-30.98	-29.1	5.96
	P₁³	97.9	1.05	1.21	0.98	28.1	9.0	40.5	20.0	2.4	71.9	3.8	nC₂₃	-33.64	-33.22	-2.30
Carb.	C	96.4	0.89	0.98	0.98	24.7	12.9	32.5	26.3	3.6	75.3	2.3	nC₂₂	-32.6 / -34.5	-34.16	-2.03
Dev.	D	94.4	2.48	2.65	0.95											
Sil.	S₂	95.1	2.31	0.07	0.99	31.0	11.9	36.9	17.6	2.1	69.0	2.6	nC₁₈	-32.53	-38.87	-6.55
Ord.	O	95.2	1.73	2.03	0.96											
Sinian	∈	92.6	0.20	0.20	0.99									-32.92	-29.15	5.9
	Zb	88.2	0.13	0.13	1.0	28.0	10.6	37.8	26.5	2.9	79.8	2.5	nC₂₃	-32.6 / -33.3	-30.48	2.99

50

Table 4. Geochemical analyses of selected natural gas samples from Sinian, Cambrian, Ordovician, and Jurassic reservoirs, Weiyuan, Longnusi, and Suinan fields, Sichuan basin (Huang and Jiang, 1986). See figures 3, 13, and 29 for the location of fields and several gas wells.

Field	Well	Stratigraphic interval	Sample depth (m)	Date of sample collection	Specific Gravity	CH_4% in whole gas	CH_4% in hydrocarbons	$C_2H_6^+$% in whole gas	$C_2H_6^+$% in hydrocarbon	H_2S%	CO_2%	$\frac{H_2S}{CO_2}$	N_2%	$\frac{CH_4}{C_2H_6^+}$	$\frac{CH_4}{C_2+C_3}$	$\frac{C_2^+}{C_1}$
Longnusi	Nu107	J_{ts}	1244.40~1266.60	1980.4.21	0.661	83.40	87.03	12.43	12.97		0.35		3.82	6.71	7.3	0.1490
Longnusi	Nu107	J_{t1-s}	1366.00~1413.40	1980.3.14	0.735	79.93	81.06	18.67	18.94		0.46		0.94	4.28	5.6	0.2336
Longnusi	Nuji well	O_1	4523.80~4534.80	1978.3.9	0.576	96.50	98.05	1.92	1.95	1.09	0.22	4.95	0.27	50	50	0.0199
Suinan		O_1	4523.80~4534.80	1978.5.3	0.579	95.94	98.19	1.77	1.81	1.34	0.48	2.79	0.47	54	54	0.0184
Suinan	Moshen 1 well	$O_1\sim O_3$	4378.00~4395.00	1979.3.22	0.618	92.78	99.76	0.22	0.24	6.00			1.00	422	422	0.0024
Suinan		$\in_1\sim\in_2$	4432.00~4475.00	1979.1.24	0.578	97.03	99.78	0.21	0.22	2.33			0.43	462	462	0.022
Longnusi	Noji well	Z_b^1	5206.00~5248.00	1977.6.30	0.600	92.82	99.94	0.06	0.06	1.04	2.49	0.42	3.59	1547	1547	0.0006
Longnusi		Z_b^1	5206.00~5248.00	1977.10.12	0.595	92.81	100	0.00	0.00	2.02			5.08	∞	∞	0.0000
Weiyuan	Weiji well	Z_b^1	2859.39	1984.10.16	0.6269	90.19	99.78	0.20	0.22	5.27			4.43	451	451	0.0022
Weiyuan		Z_b^1	2859.39	1973.9.4	0.657	84.66	99.82	0.15	0.18	2.38	6.60	0.28	5.92	564	564	0.0018

<table>
<thead>
<tr><th>Well</th><th>Sample depth (m)</th><th>CH₄ in HCs %</th><th>C₂H₆ in HCs %</th><th>H₂S%/g/m³</th><th>CO₂%/g/m³</th><th>N₂%</th><th>CH₄/ C₂H₆</th><th>H₂S/CO₂</th></tr>
</thead>
<tbody>
<tr><td>Weiji</td><td>2837.5~3041.61</td><td>84.66/99.82</td><td>0.15/0.18</td><td>2.38/36.619</td><td>6.60/130.45</td><td>5.92</td><td>564.4</td><td>0.281</td></tr>
<tr><td>2</td><td>2836.5~3005</td><td>85.07/99.87</td><td>0.11/0.13</td><td>1.31/20.159</td><td>4.86/95.99</td><td>8.33</td><td>773.4</td><td>0.210</td></tr>
<tr><td>5</td><td>2781.05~2847.87</td><td>86.16/99.86</td><td>0.12/0.14</td><td>0.74/11.418</td><td>3.94/77.92</td><td>8.68</td><td>718</td><td>0.147</td></tr>
<tr><td>10</td><td>2840~2978.68</td><td>86.66/99.87</td><td>0.11/0.13</td><td>0.98/15.057</td><td>3.69/73.0</td><td>8.23</td><td>787.8</td><td>0.206</td></tr>
<tr><td>26</td><td>2896~2975</td><td>86.62/99.86</td><td>0.12/0.14</td><td>1.21/18.554</td><td>4.63/91.60</td><td>7.15</td><td>721.8</td><td>0.203</td></tr>
<tr><td>51</td><td>2904.5~2960</td><td>86.83/99.78</td><td>0.19/0.22</td><td>0.91/14.019</td><td>4.43/87.2</td><td>8.27</td><td>457</td><td>0.161</td></tr>
<tr><td>100</td><td>2959~3041</td><td>86.8/99.85</td><td>0.13/0.15</td><td>1.18/18.180</td><td>5.07/100.1</td><td>6.47</td><td>667.7</td><td>0.182</td></tr>
<tr><td>Nuji</td><td>5206~5248</td><td>92.82/99.94</td><td>0.06/0.06</td><td>1.04/—</td><td>2.49/—</td><td>3.59</td><td>1347</td><td>0.418</td></tr>
</tbody>
</table>

Weiyuan field (Weiji, 2, 5, 10, 26, 51, 100)
Longnusi field (Nuji)

Table 5. Geochemical analyses of selected natural gas samples from Sinian carbonate reservoirs, Weiyuan and Longnusi fields, Sichuan basin (Huang and Ran, 1989). See figures 3, 13, and 29 for the location of the fields and several gas wells.
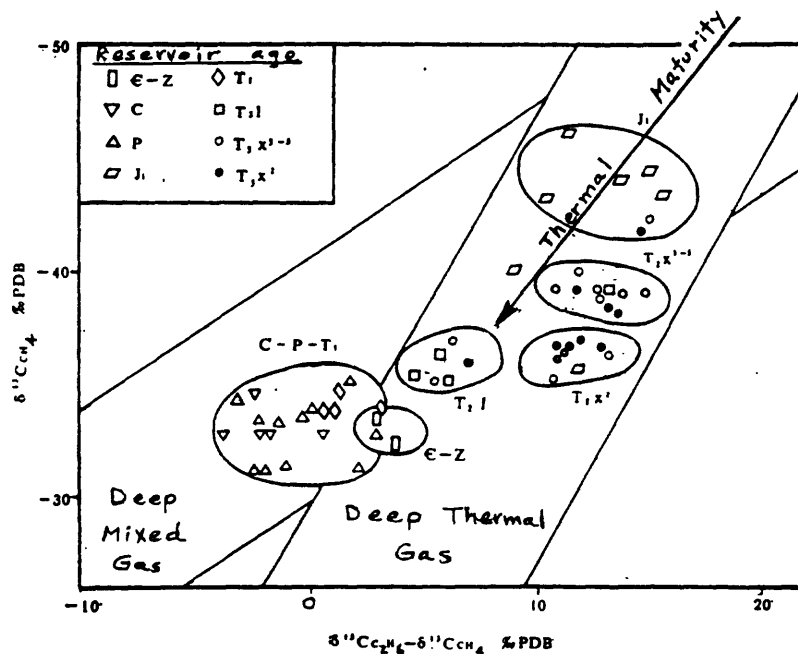
Figure 30. Plot of δ^{13}C methane vs. δ^{13}C ethane $-\delta^{13}$C methane for selected natural gas samples from the Sichuan basin (Zhang, 1986).

carbon isotopic composition of the methane (-30 to -40 per mil $\delta^{13}C$) is consistent with nonassociated gas derived from the thermal cracking of oil (Tissot and Welte, 1984). A methane $\delta^{13}C$ value of about -40 per mil generally corresponds with the bottom of the oil window. Minor to trace amounts of C_6+ compounds in the nonassociated gas provide possible additional evidence in favor of thermogenic gas derived from an oil source (Xu and Qiu, 1990). Several of the C_6^+ compounds can be traced to specific oils and oil-prone source beds (Qiu Yunyu, presentation in Wuxi, October 28, 1991). The associated gases in Jurassic reservoirs have methane $\delta^{13}C$ values lighter than -40 per mil indicating generation in the oil window.

A plot of the carbon isotopic composition of methane and ethane for selected gases--including associated gas from Jurassic reservoirs--shows a clustering of data into two general fields identified by Zhang (1986) as deep thermal mixed gas and deep thermal gas (fig. 30). The deep thermal mixed gas region of the plot contains gas from Carboniferous, Permian, and Lower Triassic reservoirs, all of which have very similar isotopic composition. Isotopic composition suggests mixing of gases from different source rocks. The deep thermal gas region of the plot, in contrast, shows a greater diversity of isotopic values but they tend to cluster in secondary groups according to reservoir age (fig. 30). The methane $\delta^{13}C$ of the gases becomes heavier with increasing age indicating an expected increasing thermal maturity with increasing age. The segregation of the gases, according to reservoir age, in the deep thermal gas field seems to emphasize the importance of regional seals.

Rice and Ryder collected gas samples from the Weiyuan No. 2 well, Weiyuan field, and from the Xinglongchang No. 3 well, Xinglongchang field (figs. 8, 13). Gas from the Weiyuan field was sampled from a Sinian carbonate reservoir at about 3,000 m whereas gas from the Xinglongchang field was sampled from the Lower Triassic Jialingjiang Formation at about 1,300 m. The results of the analyses will be presented in a later report.

PRODUCTION HISTORY AND RESOURCE ASSESSMENT

Few published data are available for cumulative production, field sizes, and assessments of undiscovered oil and gas resources in the Sichuan basin. This section cites selected published data and unpublished data learned from formal presentations in October 1991. Although far from complete, the data cited here give the reader some understanding for the magnitude of the large gas resources in the basin.

Gas has been produced from the Ziliujing field near Zigong (fig. 9) since about 280 B.C. when shallow wells were drilled (or dug) for

brine and gas extraction. Starting about 1835, gas from the field
was produced from wells that had been drilled by bamboo-constructed
rigs to depths in excess of 1000 m. Zhai and others (1987) report
that 77 gas and(or) oil fields had been discovered through 1983. A
plot of these fields by year of discovery indicates that modern
exploration drilling began about 1939 and that most fields were
discovered between 1956 and 1983 (table 6). By the early 1990's the
Sichuan basin had 100 gas fields with estimated original recoverable
gas resources of 10.5 trillion cubic feet (TCF) (Li Wenguo
presentation at Chengdu, October 7, 1991).

Ultimate recoverable gas from the giant Weiyuan field,
discovered in 1964, is estimated to be between 1.06 and 1.41 TCF of
which 455 to 480 billion cubic feet (BCF) of gas have already been
produced (Korsch and others, 1991; Madame Liu; presentation at
Weiyuan, October 19, 1991). A total of 17.5 to 18.3 million cubic
feet of gas (MMCF) per day are produced from 70 wells (Madame Liu,
presentation at Weiyuan, October 19, 1991). Meyerhoff (1970)
estimates ultimate recoverable gas from an additional 10 gas fields
in the basin, including Shiyougou-Dongxi (7 TCF), Huayingshan (3
TCF), Dengjingguan (2 TCF), Ziliujing (1 TCF), and Shengdenshan (1
TCF) (fig. 3). Also, ultimate recoverable oil from 6 oil fields in
the Sichuan basin, including Longnusi (606 million barrels) and
Nanchong (100 million barrels), is estimated by Meyerhoff (1970)
(fig. 3). Judging from the recent 10.5 TCF of ultimate recoverable
gas from the 100 gas fields discovered to date in the basin (Li
Wenguo, presentation at Chengdu, October 7, 1991), the gas estimates
of Meyerhoff (1970) are too high. Estimates of oil-field size by
Meyerhoff (1970) also are too high.

Estimated natural gas production for the Sichuan basin, from
1955 through 1968, is 2.6 TCF (Meyerhoff, 1970). According to
Meyerhoff (1970), annual production increased steadily from 4 BCF in
1955 to 200 BCF in 1963, doubled to 400 BCF between 1963-1964, and
remained at around 400 BCF through 1968. The annual natural gas
output for the Sichuan basin in 1987 was about 206.5 BCF (China Oil,
1987a). In 1991, the annual natural gas output of the basin
increased to about 245 BCF which was about half the total 1991
natural gas production for all of China (Oil and Gas Journal, 1992).
By adding Meyerhoff's (1970) 1955-1968 total production (2.6 TCF) to
the reported 1987 (.21 TCF) and 1991 (.25 TCF) annual gas production,
and to assumed annual gas production histories of 400 BCF/yr or .80
TCF (1969-1970), 300 BCF/yr (or 3.0 TCF (1971-1980), 250 BCF/yr or
1.5 TCF (1981-1986), and 210 BCF/yr or .63 TCF (1988-1990), the
cumulative gas production for the Sichuan basin through 1991 is about
9 TCF.

The Chinese Ministry of Geology and Mineral Resources (CMGMR)
recently estimated that the ultimate in-place gas resources in the
Sichuan basin are 280 TCF (Oil and Gas Journal, 1992). Mass balance
calculations of ultimate in-place gas resources by Li Wenguo (1988;
presentation at Chengdu, October 7, 1991) range between 175 and 1,750

55
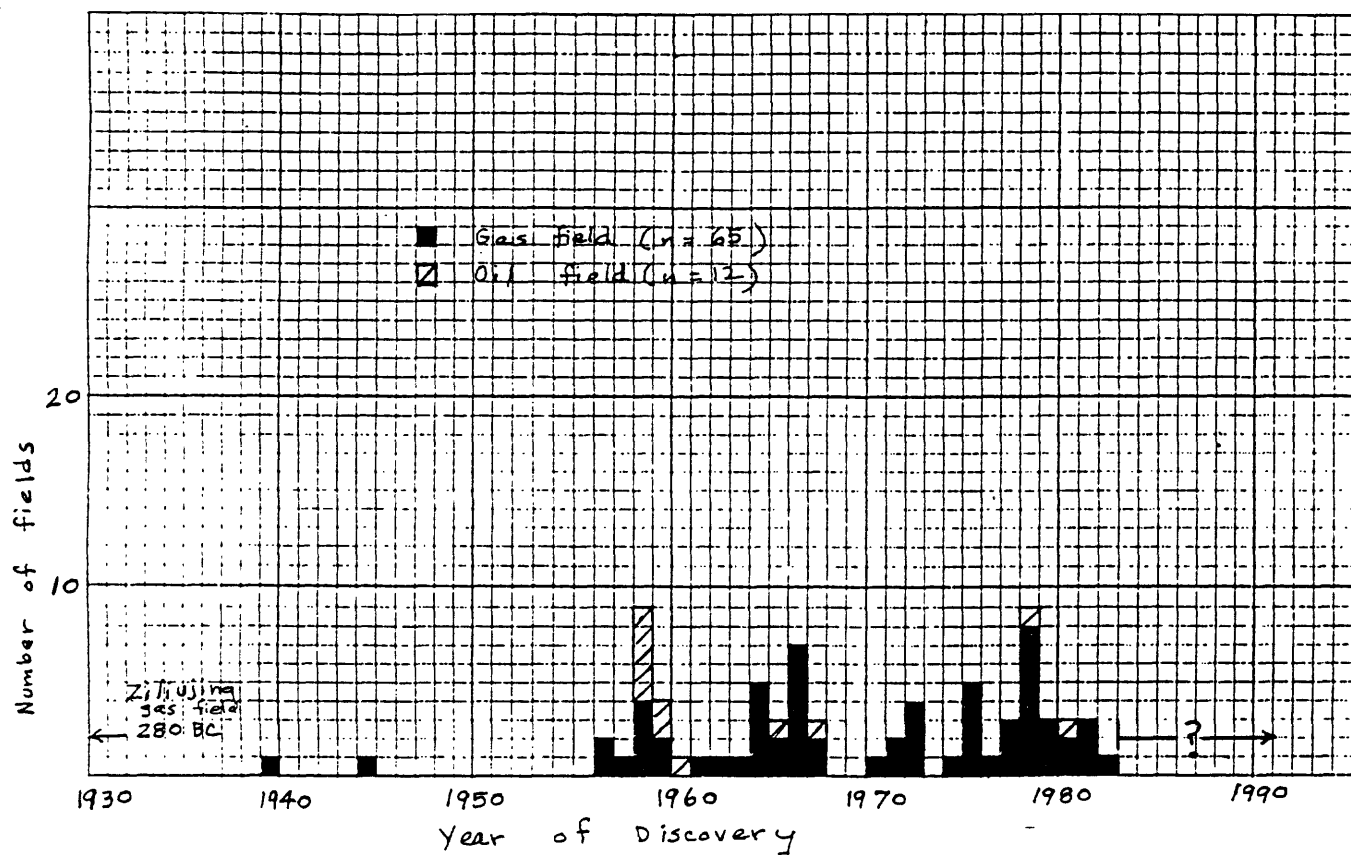
Table 6. Oil and gas fields in the Sichuan basin plotted by
year of discovery (data from Zhai and others, 1987).

56

TCF. The low estimate assumes that 1/1000 of the original gas generated is preserved, whereas the high estimate assumes that 1/100 of the original gas generated is preserved. Both the 175 TCF estimate of Li Wenguo and the 280 TCF estimate of the CMGMR seem reasonable. Given a 25 percent recovery factor and given that 10.5 TCF of the recoverable gas has already been discovered, approximately 33 to 60 TCF of recoverable undiscovered gas remains. Most of the undiscovered gas is expected from Upper Triassic tight sandstone reservoirs and from Permian and Upper Triassic coal beds.

The Chinese Central Coal Mining Research Institute (Zhang and Zhang, 1991) estimates that the in-place resources of coalbed gas in China to depths of 2,000 m are about 1,000 TCF. Very likely, a large part of this coalbed gas will come from Sichuan basin coal beds because of their high rank and very gassy character. According to Masters and others (1991), China's ultimate resources of natural gas from conventional reservoirs are 226 TCF. Therefore, if the Chinese recover 25 percent of their coalbed gas, they will have a resource about equal to their conventional gas.

CONCLUSIONS

From most indications, the potential for undiscovered natural gas resources in the Sichuan basin is good. Excellent source beds consisting of oil-prone Cambrian, Silurian, and Permian black shale and gas-prone Upper Permian and Upper Triassic coal beds have generated enormous quantities of oil and natural gas, most of which have been converted by high-temperature thermogenic reactions to dry gas. Most of the natural gas accumulated in fractured carbonate reservoirs, low-permeability sandstone reservoirs, and coal beds. There seems to be no doubt that large quantities of gas have been generated in the Sichuan basin; the question remains, however, as to how much of it has been trapped and how much can be recovered from tight sandstone reservoirs and coal beds.

Anticlines, containing gas in fractured carbonate reservoirs, have been the most common exploration target in the Sichuan basin for over 40 years because they are easily identified and because they have initially high gas yields per well. However, most of these anticlines have been drilled and their gas resources identified. Undiscovered gas accumulations may remain in those anticlines which have been inaccessible to now because of topography or whose traps have been difficult to image with earlier seismic technology. Large-scale truncation traps, although not yet proven to be productive, may be an additional source of gas in carbonate reservoirs.

Future gas resources in the basin will depend on gas trapped in unconventional reservoirs such as low-permeability Upper Triassic sandstone and Permian and Upper Triassic coal beds. These unconventional reservoirs have large in-place gas resources but their recoverability is generally lower than for conventional reservoirs. Research should be focused on the character and extent of these

unconventional reservoirs. Topics of research could include: 1) distribution of modern geothermal gradients, 2) distribution of abnormal formation pressure (over and underpressuring), 3) distribution of "sweet spots" in gas production and their causes, 4) mechanism(s) of gas storage, 5) the search for additional low-permeability reservoirs (including Sinian dolomite and Ordovician carbonates), 6) improving gas recoverability from fractured reservoirs, 7) reservoir characterization of carbonates, tight gas sandstones, and coal beds, and 8) exploration for deep gas where overpressuring, high temperatures, and non-hydrocarbon gases are common.

REFERENCES

Allen, C.R., Luo Zhuoli, Qian Hong, Wen Xueze, Zhou Huawei, and Huang Weishi, 1991, Field study of a highly active fault zone: The Xianshuihe fault of southwestern China: Geological Society of America Bulletin, v. 103, no. 9, p. 1178-1199.

Bally, A.W., Chou, I-Ming, Clayton, R., Eugster, H.P., Kidwell, S., Meckel, L.D., Ryder, R.T., Watts, A.B., and Wilson, A.A., 1986, Notes on sedimentary basins in China--Report of the American sedimentary basins delegation to the People's Republic of China: U.S. Geological Survey Open-File Report 86-327, 107 p.

Bao Ci, Yang Xianjie, and Li Dengxiang, 1985, Regional structure features and structural mode of Sichuan basin: Preprint of paper presented at Sino-American Conference on petroleum-bearing sedimentary basins (August 18-21, 1985, Zhouxian), 28 p., 15 figs.

Chen Chihliang and Chen Shihyu, 1987, Tectonic evolution of the western margin of the Yangtze block: Chengdu Institute of Geology and Mineral Resources, Chongqing Publishing House, 172 p.

Chen Huanjiang, Sun Zaucai, and Zhang Yuchang, 1986, The framework of Chinese petroliferous basins: Journal of Petroleum Geology, v. 9, no. 4, p. 451-462.

Chen Wei, Li Pengju, and Lu Huafu, 1992, The application of finite difference in the calculation in a balancing cross section--taking Zhongba gas field, northwest Sichuan Province as an example (in Chinese with English abstract): Petroleum Exploration and Development, v. 19, no. 6, p. 43-50.

Chen Yaohuang and Chen Shengji, 1982, Gas origin and exploration in Sichuan basin (in Chinese with English abstract): Natural Gas Industry, v. 1, no. 1, p. 27-34.

Chen Zongqing, 1982, The formation of Carboniferous gas pools in east Sichuan (in Chinese with English abstract): Acta Petrolei Sinica, v. 3, no. 1, p. 23-28.

China Oil, 1986, 41 proven coal gas fields in China: China Oil, v. 3, no. 4, p. 114.

China Oil, 1987a, The productivity of natural gas in Sichuan grows rapidly, in A summary of events in China's oil industry: China Oil, v. 4, no. 4, p. 85.

China Oil, 1987b, Extensive three-dimensional seismic exploration undertaken in eastern Sichuan: China Oil, v. 4, no. 1, p. 85.

59

Chou Mingkuei and Liu Yenjan, 1988, Tectonic features and geological evolution of the Xichang-central Yunnan region (in Chinese): Chengdu Institute of Geology and Mineral Resources, Chongqing Publishing House, 198 p.

Dai Jinxing, 1980, Preliminary research on natural gas in coal series in China (in Chinese with English abstract): Acta Petrolei Sinica, v. 1, no. 4, p. 27-37.

Gas field maps of China, 1987, citation unknown.

Guo Zhengwu, 1991a, Geological framework and hydrocarbon in Sichuan basin: preprint of paper presented October 7, 1991, Chengdu, 14 p., 17 figs.

Guo Zhengwu, 1991b, The sandstone gas-bearing territory in the west part of Sichuan basin: preprint of paper presented October 7, 1991, Chengdu, 11 p.

Hsü, K.J., 1989, Origin of sedimentary basins of China, in Zhu, X., ed., Chinese sedimentary basins: Elsevier, Amsterdam, p. 207-227.

Hsü, K.J., Sun Shu, and Li Jiliang, 1988, Huanan alps, not South China platform: Scientia Sinica (Series B), v. 31, no. 1, p. 109-119.

Huang Zizhong and Jiang Huaicheng, 1986, On the origin of Ordovician natural gas in Sichuan basin (in Chinese with English abstract): Acta Petrolei Sinica, v. 7, no. 4, p. 11-23.

Huang Zizhong and Ran Longhui, 1989, Bitumen and oil-gas exploration in Sinian "Denying Limestone" in Sichuan basin (in Chinese with English abstract): Acta Petrolei Sinica, v. 10, no. 1, p. 27-36.

Huang, J.Q. and others, 1976, Geological map of China (in Chinese): Publishing House of Geology, Beijing, 2 sheets, scale 1:4,000,000.

Korsch, R.J., Mai Huazhao, Sun Zhaocai, and Gorter, J.D., 1991, The Sichuan basin, southwest China: A Late Proterozoic (Sinian) petroleum province: Precambrian Research, v. 54, p. 45-63.

Kruger, D.W., 1993, International opportunities to reduce coal mine methane: Proceedings of the 1993 International Coalbed Methane Symposium, The University of Alabama/Tuscaloosa, May 17-21, 1993, p. 599-608.

Lee, K.Y. and Masters, C.D., 1988, Geologic framework, petroleum potential, and field locations of the sedimentary basins in China: U.S. Geological Survey Miscellaneous Investigations Series Map I-1952, 2 sheets, scale 1:5,000,000.

Li Wenguo, 1988, The oil/gas potential calculated by material balance and the application in geology (in Chinese with English abstract): Experimental Petroleum Geology, v. 10, no. 1, p. 1-10.

Liu Hefu, 1989, citation unavailable.

Liu Huaibo, Rigby, J.K., Li Guisen, Xia Kedong, and Liu Lingshan, 1991, Upper Permian carbonate buildups and associated lithofacies, western Hubei-eastern Sichian provinces, China: American Association of Petroleum Geologists Bulletin, v. 75, no. 9, p. 1447-1467.

Liu Huiren, 1988, Geology of Mount Emei (Emeishan), Sichuan Province, China (in Chinese): Chongqing Press, 64 p.

Lu Banggan, Yuan Bingheng, Wei Zude, Lu Yousheng, and others, 1989, Typical seismic section atlas of China (in Chinese): Petroleum Industry Press, Beijing, 260 p.

Ma Xingzhi and Wu Liusheng, 1988, Drilling engineering practice in Sichuan basin: China Oil, v. 5, nos. 3/4, p. 74-77.

Masters, C.D., Root, D.H., and Attanasi, E.D., 1991, World resources of crude oil and natural gas: Preprint of Thirteenth World Petroleum Congress, 14 p.

Meyerhoff, A.A., 1970, Developments in mainland China, 1949-1968: American Association of Petroleum Geologists Bulletin, v. 54, no. 8, p. 1567-1580.

Oil and Gas Journal, 1992, China switches E & D focus to natural gas: Oil and Gas Journal, v. 90, no. 1, p. 30 and 32.

Qiu Yunyu, Xu Lian, and others, 1986, Preliminary investigation on multiple-ringed aromatic hydrocarbon index in the correlation of oil sources in a highly evolved area (in Chinese): Central Laboratory of Petroleum Geology, Ministry of Geology and Mineral Resources, November 1986, 16 p.

Song Wenhai, 1989, citation unavailable.

Sun Zhaocai, Qiu Yunyu, and Guo Zhengwu, 1991, On the relationship of the intraplate deformation and the secondary formation of oil/gas pools--The general regularities of the oil/gas formation in marine environment of the Yangtze area (in Chinese with English abstract): Experimental Petroleum Geology, v. 13, no. 2, p. 107-142.

Terrill, Ross, 1985, Sichuan: Where China changes course: National Geographic, v. 168, no. 3, p. 280-317.

Tissot, B.P. and Welte, D.H., 1984, Petroleum formation and occurrence: Springer-Verlag, New York, 699 p.

Ulmishek, Gregory, 1993, Geology and hydrocarbon resources of onshore basins in eastern China: U.S. Geological Survey Open-File Report 93-4, 150 p.

Wang Jinqi, Bao Ci, Lou Zhili and Guo Zhengwu, 1989, Formation and development of the Sichuan basin, in Zhu, X., ed., Chinese sedimentary basins: Elsevier, Amsterdam, p. 147-163.

Xu Lian and Qiu Yunyu, 1990, Analysis method and geological application of C_6+ hydrocarbons in natural gas of high evolution areas (in Chinese with English abstract): Oil and Gas Geology, v. 11, no. 1, p. 43-50.

Xu Zhongying, 1988, The Permo-Carboniferous structural mode and hydrocarbon pool in eastern Sichuan basin (in Chinese with English abstract): Acta Petrolei Sinica, v. 9, no. 4, p. 33-40.

Yin Jiantang, 1985, Sichuan basin, in ESCAP atlas of stratigraphy IV: People's Republic of China Economic and Social Commission for Asia and the Pacific Mineral Development Series No. 52, United Nations, New York, p. 63-69.

Zhai Guangming and others, 1987, Sichuan oil and gas fields (in Chinese): Chinese Petroleum Geology, v. 10, Petroleum Industry Press, Beijing, 516 p.

Zhang, Xinmen and Zhang Sui An, 1991, Coalbed methane in China (in Chinese with English abstract): Xian Branch, Central Coal Mining Research Institute, 145 p.

Zhang Yigang, 1986, Methods for distinguishing carbon isotopes in natural gases and their applications (in Chinese): Central Laboratory of Petroleum Geology, Ministry of Geology and Mineral Resources, 20 p.

APPENDIX A.

American Participants

Dudley D. Rice, Delegation Chairman   U.S. Geological Survey
                                         Box 25046, MS 971
                                         Denver Federal Center
                                         Denver, Colorado 80225

Robert T. Ryder   U.S. Geological Survey
                                         National Center, MS 955
                                         Reston, Virginia 22092

Chinese Participants

Sun Zhaocai, Delegation Chairman   Central Lab of Petroleum
Professor and Director   Geology
                                         Ministry of Geology and
                                             Mineral Resources
                                         P. O. Box 916
                                         Wuxi, Jiangsu 214151
                                         People's Republic of China

Chen Zhaoguo   Southwest China Bureau of
Geologist   Petroleum Geology
                                         Research Party of Petroleum
                                             Geology
                                         Ministry of Geology and
                                             Mineral Resources
                                         Qinglongchang
                                         Chengdu, Sichuan 610081
                                         People's Republic of China

Deng Kangling   Southwest China Bureau of
Senior Geologist, Professor   Petroleum Geology
                                         Research Party of Petroleum
                                             Geology
                                         Ministry of Geology and
                                             Mineral Resources
                                         Qinglongchang
                                         Chengdu, Sichuan 610081
                                         People's Republic of China

Feng Fukai   Institute of Petroleum Geology
Senior Research Fellow   Ministry of Geology and
                                             Mineral Resources
                                         20 Chengfu Road
                                         Beijing 100083
                                         People's Republic of China

63

Guo Zhengwu
Chief Geologist
Professor

Southwest China Bureau of
    Petroleum Geology
Ministry of Geology and
    Mineral Resources
No. 116, North Section 4
Yihuan Road
Chengdu, Sichuan 610081
People's Republic of China

Jiang Shijin
Program Official

Department of International
    Cooperation
Ministry of Geology and
    Mineral Resources
Xisi, Beijing 100812
People's Republic of China

Li Wenguo
Senior Geologist

Southwest China Bureau of
    Petroleum Geology
Research Party of Petroleum
    Geology
Ministry of Geology and
    Mineral Resources
Qinglongchang
Chengdu, Sichuan 610081
People's Republic of China

Liu Madame
Senior Geologist

Southwest Bureau
China National Petroleum
    Corporation
Zigong, Sichuan
People's Republic of China

Liu Yingkai
Senior Geologist

Southwest China Bureau of
    Petroleum Geology
Research Party of Petroleum
    Geology
Ministry of Geology and
    Mineral Resources
Qinglongchang
Chengdu, Sichuan 610081
People's Republic of China

Mai Huazhao
Senior Petroleum Geologist,
Director of Department of
  Sedimentology

Central Lab of Petroleum Geology
Ministry of Geology and
    Mineral Resources
P. O. Box 916
Wuxi, Jiangsu 214151
People's Republic of China

Qiu Yunyu
Senior Geologist

Central Lab of Petroleum
    Geology
Ministry of Geology and
    Mineral Resources
P. O. Box 916
Wuxi, Jiangsu 214151
People's Republic of China

Sun Renyi
Deputy Director

Department of International
    Cooperation
Ministry of Geology and
    Mineral Resources
64 Funei Dajie
Xisi, Beijing
People's Republic of China

Wang Fuqing
Deputy Director

Institute of Petroleum Geology
Ministry of Geology and
    Mineral Resources
20 Chengfu Road
Beijing 100083
People's Republic of China

Yin Jiantang
Senior Geologist

Southwest China Bureau of
    Petroleum Geology
Research Party of Petroleum
    Geology
Ministry of Geology and
    Mineral Resources
Qinglongchang
Chengdu, Sichuan 610081
People's Republic of China

Zhang Wencheng
Head of the Science and
    Technology Information Department

Central Lab of Petroleum
    Geology
Ministry of Geology and
    Mineral Resources
P. O. Box 916
Wuxi, Jiansu 214151
People's Republic of China

Zhang Yigang
Professor and Director of
    Geochemistry Division

Central Lab of Petroleum
    Geology
Ministry of Geology and
    Mineral Resources
P. O. Box 916
Wuxi, Jiangsu 214151
People's Republic of China

Zheng Shuiji
Junior Research Fellow

Institute of Petroleum Geology
Information Section
Ministry of Geology and
    Mineral Resources
20 Chengfu Road
Beijing 100083
People's Republic of China

APPENDIX B

Presentations in Beijing, October 5, 1991

(listed in order of presentation)

Wang Fuqing	Organization and activities of Institute of Petroleum Geology
Feng Fukai	Structure, thermal fields, and distribution of oil and gas in hydrocarbon-bearing basins of China

Presentations in Chengdu, October 7, 1991
(listed in order of presentation)

Guo Zhengwu	Petroleum geology of the Sichuan basin
Liu Yingkai	Interpretation of deep crustal, 1000-km-long seismic profile through the Sichuan basin
Li Wenguo	Assessment of oil and gas resources in the Sichuan basin
Yin Jiantang	Petroleum geology of the Jurassic and Cretaceous sequence, Sichuan basin
Deng Kangling	Evolution of the Sichuan basin

Presentations in Chengdu, October 8, 1991
(listed in order of presentation)

Dudley D. Rice	Distribution, character, and origin of deep gas (>4.5 km deep) in the United States
	Coalbed gas resources in the United States
Robert T. Ryder	Petroleum geology of the Appalachian basin, eastern United States
	Character and origin of oil in Cambrian reservoirs, Appalachian basin, United States

Presentations in Zigong, October 19, 1991

Liu Madame	Petroleum geology and production history of the Weiyuan gas field

Presentations in Wuxi, October 28, 1991
(listed in order of presentation)
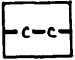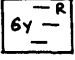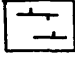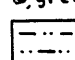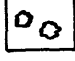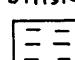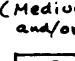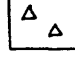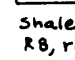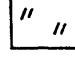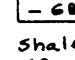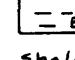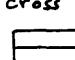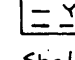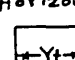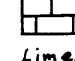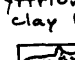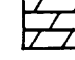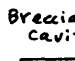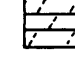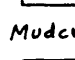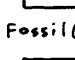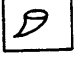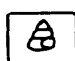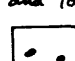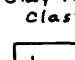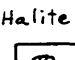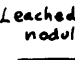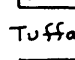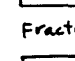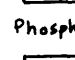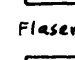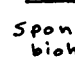
Sun Zhaocai	Tectonic evolution of the Yangtze platform
Qiu Yunyu	Origin of hydrocarbons on the Yangtze platform
Chai Liguo	Structure and tectonics of the Longmenshan
Zhang Yigang	Distribution, character, and origin of natural gas in China

Presentations in Wuxi, October 29, 1991
(listed in order of presentation)

Dudley D. Rice	Natural gas fields in the foreland basins of the Rocky Mountains, United States
	Distribution, character, and origin of deep gas (>4.5 km deep) in the United States
Robert T. Ryder	Petroleum geology of the Appalachian basin, eastern United States

Dominant Lithology

Conglomerate	Coal
Breccia	Basalt
Sandstone	
Sandstone (R,red; G,green)	
Siltstone	
Shale (Medium gray and/or green)	
Shale (R, red; RB, red brown)	
Shale (G, green; GB, green brown)	
Shale (black)	
Shale (yellow)	
Limestone (R, reddish)	
Dolomite	
Dedolomite	
Dolomite (sucrosic)	

Lithologic Modifiers

Sandy	Coral
Argillaceous (Gy, gray; R, red)	Productid brachiopod
Calcareous	Ammonite
Vug's	Gastropod
Oolitic	Brachiopod
Cherty	Wood fragments and logs
Evaporite mineral(s)	Clay rip-up clasts
Medium-scale cross beds	Halite crystals
Horizontal beds	Leached evaporite nodules
Yttrium-bearing clay bed	Tuffaceous
Breccia-filled cavity	Fractures
Mudcracks	Phosphate bed
Fossil (undefined)	Flaser beds
Crinoid fragments	Sponge bioherm
Silty	Ripple marks

Other

● Oil reservoir in subsurface

☼ Gas reservoir in subsurface

Oil or bitumen stain

Source rock

R_o(%) Vitrinite reflectance (in percent)

TOC Total organic carbon (in weight percent)

〜 Unconformity

← Sample G-12 Sample(s) collected by Rice and Ryder

Thrust fault

φ Porosity

Appendix C. Explanation of lithologic symbols used in figures 16-19.